

1 **Coccolithophore biodiversity controls carbonate export in the Southern Ocean**

2 Andrés S. Rigual Hernández^{1,*} Thomas W. Trull^{2,3}, Scott D. Nodder⁴, José A. Flores¹,
3 Helen Bostock^{4,5}, Fátima Abrantes^{6,7}, Ruth S. Eriksen^{2,8}, Francisco J. Sierro¹, Diana M.
4 Davies^{2,3}, Anne-Marie Ballegeer⁹, Miguel A. Fuertes⁹, and Lisa C. Northcote⁴.

5 1 Área de Paleontología, Departamento de Geología, Universidad de Salamanca, 37008
6 Salamanca, Spain

7 2 CSIRO Oceans and Atmosphere Flagship, Hobart, Tasmania 7001, Australia

8 3 Antarctic Climate and Ecosystems Cooperative Research Centre, University of
9 Tasmania, Hobart, Tasmania 7001, Australia

10 4 National Institute of Water and Atmospheric Research, Wellington 6021, New Zealand

11 5 University of Queensland, Brisbane, Queensland 4072, Australia

12 6 Portuguese Institute for Sea and Atmosphere (IPMA), Divisão de Geologia Marinha
13 (DivGM), Rua Alferedo Magalhães Ramalho 6, Lisboa, Portugal

14 7 CCMAR, Centro de Ciências do Mar, Universidade do Algarve, Campus de Gambelas,
15 8005-139 Faro, Portugal

16 8 Institute for Marine and Antarctic Studies, University of Tasmania, Private Bag 129,
17 Hobart, Tasmania 7001, Australia

18 9 Departamento de Didáctica de las Matemáticas y de las Ciencias Experimentales,
19 Universidad de Salamanca, 37008 Salamanca, Spain.

20 * Corresponding author

21 **Abstract**

22 Southern Ocean waters are projected to undergo profound changes in their
23 physical and chemical properties in the coming decades. Coccolithophore blooms in the
24 Southern Ocean are thought to account for a major fraction of the global marine calcium
25 carbonate (CaCO₃) production and export to the deep sea. Therefore, changes in the
26 composition and abundance of Southern Ocean coccolithophore populations are likely to
27 alter the marine carbon cycle, with feedbacks to the rate of global climate change.
28 However, the contribution of coccolithophores to CaCO₃ export in the Southern Ocean is
29 uncertain, particularly in the circumpolar Subantarctic Zone that represents about half of
30 the areal extent of the Southern Ocean and where coccolithophores are most abundant.
31 Here, we present measurements of annual CaCO₃ flux and quantitatively partition them
32 amongst coccolithophore species and heterotrophic calcifiers at two sites representative

33 of a large portion of the Subantarctic Zone. We find that coccolithophores account for a
34 major fraction of the annual CaCO_3 export with highest contributions in waters with low
35 algal biomass accumulations. Notably, our analysis reveals that although *Emiliana*
36 *huxleyi* is an important vector for CaCO_3 export to the deep sea, less abundant but larger
37 species account for most of the annual coccolithophore CaCO_3 flux. This observation
38 contrasts with the generally accepted notion that high PIC accumulations during the
39 austral summer in the subantarctic Southern Ocean are mainly caused by *E. huxleyi*
40 blooms. It appears likely that the climate-induced migration of oceanic fronts will initially
41 result in the poleward expansion of large coccolithophore species increasing CaCO_3
42 production. However, subantarctic coccolithophore populations will eventually diminish
43 as acidification overwhelms those changes. Overall, our analysis emphasizes the need for
44 species-centred studies to improve our ability to project future changes in phytoplankton
45 communities and their influence on marine biogeochemical cycles.

46

47 **1. Introduction**

48 The emissions of carbon dioxide (CO_2) into the atmosphere by anthropogenic
49 industrial activities over the past 200 years are inducing a wide range of alterations in the
50 marine environment (Pachauri et al., 2014). These include ocean warming, shallowing
51 of mixed layer depths, changes in nutrient supply to the photic zone, and decreasing
52 carbonate-ion concentrations and pH of the surface ocean, a process known as ocean
53 acidification (Rost and Riebesell, 2004; Stocker et al., 2014). Substantial evidence from
54 CO_2 manipulation experiments indicates that many species of corals, pteropods,
55 planktonic foraminifera and coccolithophores will reduce their calcification rates under
56 future ocean acidification scenarios (Bijma et al., 2002; Langdon and Atkinson, 2005
57 among others; Orr et al., 2005; Bach et al., 2015; Meyer and Riebesell, 2015). Owing to
58 their moderate alkalinity and cold temperatures, Southern Ocean waters are projected to
59 become undersaturated with respect to aragonite no later than 2040 and to calcite by the
60 end of the century (Cao and Caldeira, 2008; McNeil and Matear, 2008; Shadwick et al.,
61 2013). This decline in the saturation state of carbonate, together with other changes in
62 carbonate chemistry speciation, will enhance dissolution of both aragonite and calcite
63 shells and will make the biological precipitation of carbonate difficult in some marine
64 calcifying organisms (Fabry et al., 2008; Gattuso and Hansson, 2011). Since such
65 thresholds will be reached sooner in polar regions, Southern Ocean ecosystems have been

66 proposed as bellwethers for prospective impacts of ocean acidification on marine
67 organisms at mid and low latitudes (Fabry et al., 2009).

68 Cocolithophores are a major component of phytoplankton communities in the
69 Southern Ocean, particularly in its northern-most province, the Subantarctic Zone, where
70 they often exhibit maximum abundances and diversity (e.g. Gravalosa et al., 2008;
71 Saavedra-Pellitero et al., 2014; Malinverno et al., 2015; Charalampopoulou et al., 2016).
72 Cocolithophores play an important and complex role in the Southern Ocean carbon cycle
73 (Salter et al., 2014). On the one hand, the production of calcite platelets (termed
74 coccoliths) decreases the alkalinity of surface waters thereby reducing the atmospheric
75 uptake of CO₂ from the atmosphere into the surface ocean. On the other hand, the
76 production of organic matter through photosynthesis, and its subsequent transport to
77 depth in settling particles, enhances carbon sequestration via the biological carbon pump
78 (Volk and Hoffert, 1985). Additionally, due to their high density and slow dissolution,
79 coccoliths act as an effective ballast for organic matter, increasing organic carbon
80 sequestration depths (Buitenhuis et al., 2001; Boyd and Trull, 2007; Ziveri et al., 2007).
81 Therefore, changes in the abundance, composition and distribution of coccolithophores
82 could have an extensive impact on ocean nutrient stoichiometry, carbon sequestration,
83 and nutrition for higher trophic levels in the Southern Ocean (Deppeler and Davidson,
84 2017).

85 The remoteness and vastness of the Southern Ocean, together with the inherent
86 temporal and spatial variability of pelagic ecosystems, hampers accurate characterization
87 and quantification of Southern Ocean phytoplankton communities. Advances in satellite
88 technology and modelling algorithms have allowed a circumpolar and year-round
89 coverage of the seasonal evolution of major phytoplankton functional groups within the
90 Southern Ocean (e.g. Alvain et al., 2013; Hopkins et al., 2015; Rousseaux and Gregg,
91 2015). In particular, ocean-colour satellite reflectance observations have been used to
92 quantitatively estimate coccolithophore Particulate Inorganic Carbon (PIC)
93 concentrations throughout the Southern Ocean (Gordon et al., 2001; Balch et al., 2005b).
94 These satellite estimates suggest apparent high PIC values during summer near the major
95 Southern Ocean fronts attributed to coccolithophores (Balch et al., 2011; Balch et al.,
96 2016). This band of elevated reflectance and PIC that encircles the entire Southern Ocean
97 was termed the “Great Calcite Belt” by these authors. However, comparison of satellite
98 remote-sensing data with ship-based observations (Holligan et al., 2010; Trull et al.,

99 2018) indicate that satellite ocean-colour-based PIC estimates could be unreliable,
100 particularly in Antarctic waters where they erroneously suggests high PIC abundances.
101 Shipboard observations, on the other hand, provide a detailed picture of phytoplankton
102 community composition and structure, but are dispersed, both temporally and
103 geographically, and provide rather heterogenous data in terms of taxonomic groups
104 investigated, and the sampling scales and methodologies used (e.g. Kopczynska et al.,
105 2001; de Salas et al., 2011; Poulton et al., 2013; Patil et al., 2017, among others). *In situ*
106 year-round monitoring of key strategic regions is critically needed to establish baselines
107 of phytoplankton community composition and abundance and to validate and improve
108 ocean biogeochemical models (Rintoul et al., 2012). This information is also essential if
109 we are to detect possible climate-driven changes in the structure of phytoplankton
110 communities that could influence the efficiency of the biological carbon pump, with
111 consequent feedbacks to the rate of deep-water carbon sequestration and global climate
112 change (Le Quéré et al., 2007; Deppeler and Davidson, 2017).

113 Here, we document coccolithophore and carbonate particle fluxes collected over
114 a year by four sediment trap records deployed at two strategic locations of the Australia
115 and New Zealand sectors of the Southern Ocean considered representative of a large
116 portion of the SAZ (See section 2.2 for further details). Our measurements provide
117 coccolith mass estimates of the main coccolithophore species and quantitatively partition
118 annual carbonate fluxes amongst coccolithophore species and heterotrophic calcifiers.
119 We find that coccolithophores are a major vector for CaCO₃ export out of the mixed layer
120 and that the largest contribution to CaCO₃ export is not from the most abundant species
121 *Emiliania huxleyi* but rather from larger coccolithophores species with substantially
122 different physiological traits (e.g. *Calcidiscus leptoporus*). Our results emphasize the
123 urgent need for diagnostic fitness response experiments on other coccolithophore species
124 aside from *E. huxleyi* (e.g. Feng et al., 2017) in order to be able to be able to predict the
125 impacts of anthropogenically induced changes in Southern Ocean ecosystems and
126 biological carbon uptake mechanisms.

127

128 **2. Material and methods**

129

130 **2.1 Oceanographic setting**

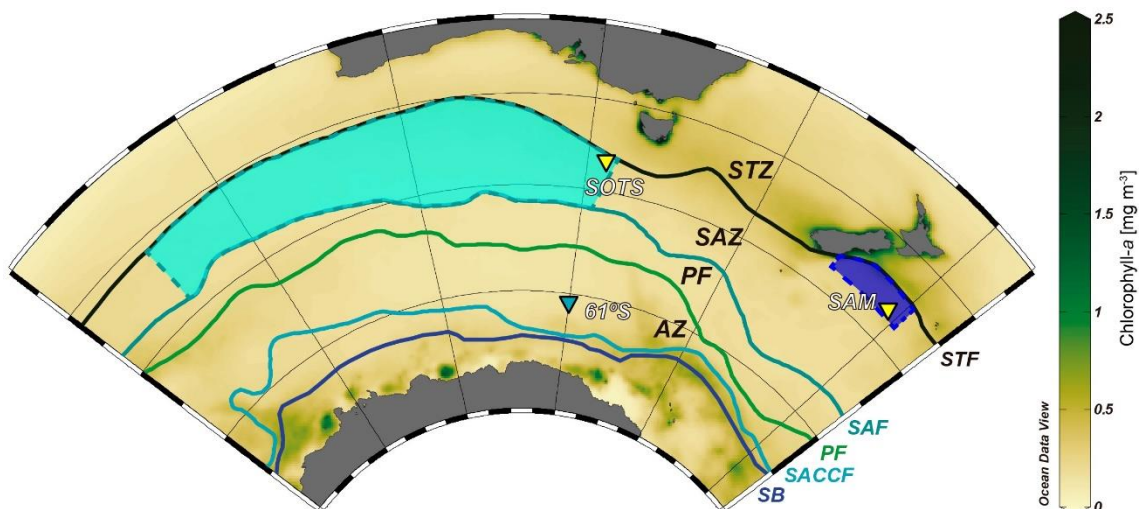
131 The SAZ alone accounts for more than half of the Southern Ocean area (Orsi et
132 al., 1995) and represents a transitional boundary between the warm, oligotrophic waters
133 of the subtropical gyres to the north and the cold, silicate-rich waters south of the Polar
134 Front (PF). The SAZ is arguably the largest high nutrient, low chlorophyll (HNLC)
135 province in the world's ocean and is central to the linkages between the ocean–
136 atmosphere CO₂ exchange and climate. The deep winter convection in the SAZ, which
137 exceeds 400 m, results in the formation of a high-oxygen water masses known as
138 Subantarctic Mode and Antarctic Intermediate Waters that connect the upper and lower
139 limbs of the global overturning circulation (Sloyan and Rintoul, 2001a, b). The formation
140 of these water masses are responsible for the sequestration of a large fraction of
141 anthropogenic CO₂ (Sabine et al., 2004), with an estimated 1 Gt C yr⁻¹ transported to
142 intermediate depths annually (Metzl et al., 1999). Macronutrient concentrations display
143 pronounced seasonal changes in the SAZ with fully replete levels during winter to
144 substantial depletion during summer, particularly for silicate (Dugdale et al., 1995;
145 Rintoul and Trull, 2001; Bowie et al., 2011). Phytoplankton community in the
146 subantarctic zone is dominated by pico- and nanoplankton including cyanobacteria,
147 coccolithophores and autotrophic flagellates with lower abundances of diatoms than polar
148 waters south the Polar Front (Chang and Gall, 1998; Kopczynska et al., 2001; de Salas et
149 al., 2011; Rigual-Hernández et al., 2015b; Eriksen et al., 2018).

150

151 **2.2 Field experiments**

152 Here we report on the coccolithophore and biogeochemical fluxes collected over
153 a year at the Australian Southern Ocean Time Series (SOTS) observatory (Trull et al.,
154 2010) and the New Zealand Subantarctic Mooring (SAM) site (Nodder et al., 2016) (Fig.
155 1). The SOTS observatory is located in the abyssal plane of the central SAZ
156 approximately 530 km southwest of Tasmania (46° 56' S, 142° 15' E) within an anti-
157 cyclonic gyre in a region characterized by weak circulation (Trull et al., 2001; Herraiz-
158 Borreguero and Rintoul, 2011). SOTS was equipped with three vertically moored, conical
159 time-series sediment traps (McLane Parflux Mk 7G-21) placed at ~1000, 2000 and 3800
160 m depth between August 2011 until July 2012. The physical, chemical and biological
161 parameters of SOTS site are regarded as representative for large portion of the Indian and
162 Australian sectors of the SAZ (~90°E and 140°E; Trull et al., 2001). The SAM site is
163 located in the Bounty Trough in in the subantarctic waters south east of New Zealand

164 (46°40'S, 178° 30'E) and was equipped with conical, time-incremental sediment trap
165 (McLane PARFLUX Mk7G-21) placed at 1500 m depth, with samples used in the present
166 study collected between November 2009 until November 2010. The SAM site is
167 considered to be representative of a wide area of the northern sector of the SAZ off eastern
168 New Zealand, approximately 171°E to 179°W and 45 to 47°S (Law et al., 2014; Fig. 1).
169 Full details of the field experiments from these two localities in the Australian and New
170 Zealand sectors of the SAZ can be found in Trull et al. (2001) and Nodder et al. (2016),
171 respectively.



172

173 **Figure 1:** Chlorophyll-*a* composite map of the Australian-New Zealand sector of the
174 Southern Ocean (July 2002 to July 2012) from the MODIS Aqua Sensor showing the
175 location of the sediment trap moorings sites: SOTS, 61°S and SAM. The regions for
176 which the SOTS and SAM sites are representative are marked with light and dark blue
177 areas, respectively. Abbreviations: Subtropical Zone – STZ, Subtropical front - STF,
178 Subantarctic Zone – SAZ, Subantarctic Front - SAF, Polar Frontal Zone - PFZ, Polar
179 Front - PF, Antarctic Zone – AZ, Southern Antarctic Circumpolar Current Front –
180 SACCF, southern boundary of the ACC – SB. Oceanic fronts after Orsi et al. (1995).
181 Ocean Data View software (Schlitzer, 2018) was used to generate this figure.

182 2.3 Sample processing

183 In short, the recovered trap bottles were refrigerated upon recovery and then
184 allowed to settle. The sample slurry was then wet-sieved through a 1 mm screen in the
185 case of SOTS (no attempt to extract zooplankton "swimmers" was made for the <1 mm
186 fraction analysed here) and through a 200 µm sieve to remove "swimmers" for the SAM

187 site. The remaining fraction was then split using a McLane wet sample divider; the SOTS
188 samples were subdivided into one tenth aliquots while one fifth splits were made for the
189 SAM samples. For the SOTS samples, a total of 55 samples were processed for calcareous
190 nannoplankton analysis. The one-tenth splits dedicated to phytoplankton analysis were
191 further subdivided into four aliquots with the McLane splitter. One aliquot was used for
192 calcareous nannoplankton analysis and the remaining three were kept refrigerated for
193 biomarker and non-calcareous microplankton analyses. In the case of the SAM samples,
194 the one-fifth aliquots were further subdivided into five subsplits, and one of those was
195 used for calcareous nannoplankton analysis. Two different types of glass slides per
196 sample were prepared. The first preparation was used for the estimation of coccosphere
197 and calcareous dinocyst (calcispheres of thoracosphaerids) fluxes and for coccolith
198 imaging. A volume ranging between 1000 and 5000 μl of the raw sample was mounted
199 on a glass slide using Canada balsam following Flores and Sierro (1997). This technique
200 produces random settling of the coccoliths for microscopic identification and
201 enumeration. The second type of glass slide was prepared following a modified protocol
202 for non-destructive disintegration of aggregates modified from Bairbakhish et al. (1999).
203 The objective of this chemical treatment is to reduce biases in the coccolith flux
204 estimations associated with the presence of different types of aggregates and
205 coccospheres (Bairbakhish et al., 1999). In brief, 2000 μl were extracted from the aliquot
206 for calcareous nannoplankton analysis and then treated with a solution comprising 900 μl
207 sodium carbonate and sodium hydrogen carbonate, 100 μl ammonia (25%) and 2000 μl
208 hydrogen peroxide (25%). The sample was agitated for 10 seconds every 10 minutes and
209 this process was repeated over an hour. Then, the reaction was stopped with catalase
210 enzyme and samples were allowed to settle for at least 48 hours before preparation on
211 microscope slides. pH controls indicate that the solution kept pH levels near 9, therefore
212 precluding coccolith dissolution. Finally, trap samples were mounted on microscope
213 slides following the same decantation method as used for the first type of glass slides (i.e.
214 Flores and Sierro, 1997).

215 **2.4 Determination of CaCO_3 fluxes**

216 A detailed description of the geochemical analytical procedures for the SOTS
217 samples is provided in Trull et al. (2001) and Rigual-Hernández et al. (2015a) while more
218 detailed procedures of the SAM trap can be found in Nodder et al. (2016). In short, for
219 the SOTS site three of the one tenth splits were filtered onto 0.45 pore size filters. Then

220 the material was removed from the filter as a wet cake of material, dried at 60°C, and
221 ground in an agate mortar. This material was used to determine the total mass and
222 composition of the major components of the flux. Particulate inorganic Carbon (PIC)
223 content was measured by closed system acidification with phosphoric acid and
224 coulometry. For the SAM site, one-fifth split was analysed for elemental calcium (Ca)
225 concentration using ICP-MS techniques. The samples were oven-dried, digested in
226 nitric/hydrochloric acid and then analysed according to the methods under US EPA 200.2.
227 Ca was used to estimate CaCO₃ content in the samples assuming a 1:1 molar ratio in
228 CaCO₃.

229

230 **2.5 Quantification and characterization of coccolithophore sinking assemblages**

231 Qualitative and quantitative analyses of coccospheres and coccoliths were
232 performed using a Nikon Eclipse 80i polarised light microscope at 1000 x magnification.
233 The taxonomic concepts of Young et al. (2003) and the Nannotax website (Young et al.,
234 2019) were used. A target of 100 coccospheres and 300 coccoliths was established;
235 however, owing to the pronounced seasonality in coccolithophore export, there were
236 some periods with very low abundance of coccospheres in the samples and therefore the
237 target of 100 coccospheres was not always met. Coccosphere and coccolith species counts
238 were then transformed into relative abundances and daily fluxes using the following
239 formula:

240

$$241 \quad F = \frac{N \times \frac{A}{n \times a} \times V \times S}{d \times T}$$

242

243 where F = coccolith flux, N = number of coccoliths, A = area of the Petri dish, n
244 = number of fields of view, a = area of a field of view, V = dilution volume, S = sample
245 split, d = number of days of collection and T = sediment trap aperture area.

246

247 **2.6 Determination of coccolith mass and size**

248 Birefringence and morphometric methods are the two most commonly used
249 approaches for estimating the calcite content of isolated coccoliths. The circularly-
250 polarized light-microscopy-based technique (Fuertes et al., 2014) is based on the
251 systematic relationship between the thickness of a given calcite particle (in the thickness

252 range of 0 - 1.55 mm) and the first-order polarization colours that it displays under
253 polarized light (Beaufort, 2005; Beaufort et al., 2014; Bolton et al., 2016). The advantages
254 of this approach are that: (i) it directly measures complete coccoliths with no assumptions
255 regarding their shape or thickness and (ii) it allows for quantification of calcite losses
256 associated with missing parts or etching of the coccoliths. Disadvantages of this technique
257 are the errors associated with the coccolith-calcite calibration and their consequent effect
258 on the coccolith mass estimates (Fuertes et al., 2014; González Lemos et al., 2018). The
259 morphometric approach, on the other hand, allows better taxonomic identification of the
260 coccoliths and has smaller errors in the length measurements (~0.1 to 0.2 μm ; Poulton et
261 al. 2011). However, this method does not allow direct measurement of coccolith thickness
262 and assumes identical shape and width proportions for all specimens of the same species,
263 among other uncertainties (see Young and Ziveri, 2000 for a review). Since the two
264 methods have different associated errors (Poulton et al., 2011), we applied both
265 approaches to our coccolith flux data in order to obtain two independent estimates of the
266 fractional contribution of coccolithophores species to total carbonate export in the SAZ.

267 For the birefringence-based approach, a minimum of 50 coccoliths of each of the
268 main coccolithophore species were imaged using a Nikon Eclipse LV100 POL light
269 microscope equipped with circular polarisation and a digital camera (Nikon DS-Fi1 8-bit
270 colour). The only exception was *E. huxleyi* for which coccolith mass values had already
271 been estimated in all the same samples at high resolution by Rigual-Hernández et al.
272 (under review). For the minor components of the flux assemblage, a lower number of
273 coccoliths were measured (Table 1). A photograph of the same apical rhabdolith of the
274 genus *Acanthoica* was taken and used for calibration at the beginning of each imaging
275 session during which microscopy light and camera settings were kept constant. A
276 different number of fields of view of multiple samples representative of different seasons
277 were photographed until the target number of coccoliths for each species was reached.
278 Photographs were then analysed by the image processing software C-Calcita. The output
279 files for single coccoliths were visually selected and classified into the lowest possible
280 taxonomic level. Length and weight measurements were automatically determined by C-
281 Calcita software. Morphometric measurements of all the species are summarized in Table
282 1. For further methodological details see Fuertes et al. (2014) and Bolton et al. (2016).

283 The second approach consisted of performing morphometric measurements on the
284 coccoliths followed by the estimation of their coccolith mass assuming a systematic

285 relation between length and thickness (Young and Ziveri, 2000). Young and Ziveri (2000)
286 proposed that the calcite content of a given coccolith could be estimated using the
287 following formula:

$$288 \text{Coccolith calcite (pg)} = 2.7 \times k_s \times l^3$$

289 where 2.7 is the density of calcite (CaCO_3 ; $\text{pg } \mu\text{m}^3$), “ k_s ” is a shape constant that varies
290 between species and morphotypes and whose value is based on the reconstruction of
291 coccolith cross profiles and “ l ” is the distal shield length (DSL). In order to undertake
292 coccolith measurements on the same coccoliths used for the birefringence-based
293 approach, we employed the distal shield length values measured by C-Calcita using
294 circularly polarized light instead of morphometric measurements on Scanning Electron
295 Micrographs (SEM) as made in Young and Ziveri (2000).

296 Since coccolith distal shield length (DSL) has been reported to be systematically
297 underestimated using cross-polarized light microscopy (e.g. D’Amario et al., 2018), we
298 evaluated the possible errors in the DSL measurements made by C-Calcita. For this
299 assessment, we measured 40 detached coccoliths of *C. leptoporus* under the SEM from
300 samples of the SOTS sediment traps using the image processing software Image-J.
301 Average DSL measurements under the SEM were then compared with those made by C-
302 Calcita on 40 randomly selected *C. leptoporus* coccoliths. The average coccolith length
303 obtained with the SEM analysis (6.37 ± 1.02 , $n = 40$) was ~ 4% shorter than that estimated
304 with C-Calcita (6.62 ± 1.47 , $n = 40$). Therefore, we assumed the error for the DSL
305 measurements with circularly polarized light is < 5%. Given the low numbers of the rest
306 of species in the samples we considered that this error is applicable for the rest of the taxa
307 measured in the current study. The subtle differences in coccolith distal length
308 measurements between techniques are most likely due to the fact that the peripheral limit
309 of the coccolith shield under the circularly-polarized light microscope (LM) is not as sharp
310 as is the case for SEM images. It follows that differences in DSL measurements between
311 SEM and LM techniques will be likely similar or smaller in the case of larger species.
312 Since the majority of coccolith species identified in the current study display a similar
313 (e.g. *Gephyrocapsa oceanica*, *Syracosphaera pulchra*, *Umbellosphaera tenuis* and
314 *Umbicosphaera sibogae*) or larger size (e.g. *Coccolithus pelagicus* and *Helicosphaera*
315 *carteri*) than *C. leptoporus*, it could be assumed that the <5% error on DSL estimates for
316 *C. leptoporus* is applicable for the rest of the species found in the current study. For the
317 k_s value of each taxa, data from the literature was employed (Table 1). *E. huxleyi*

318 assemblages in the SAZ are composed of a mixture of five different morphotypes: A, A
319 overcalcified, B, B/C and C, each of which is characterized by different shape factors (k_s).
320 Since k_s is not available for all the morphotypes found in the SAZ and it is not possible
321 to differentiate between morphotypes in our light microscopy images, we used the mean
322 shape factor constant for *E. huxleyi* (i.e. $k_s = 0.0275$) to provide a range of coccolith mass
323 estimates for this species (Table 1 and Fig. 4).

324 **2.7 Calculation of annual estimates**

325 Since the trap collection periods encompassed a period shorter than a calendar
326 year, annual estimates of coccolith and CaCO_3 fluxes and species relative abundances had
327 to be estimated. For the SOTS site, a total of 336 days were sampled for the 1000 and
328 2000 m traps and 338 days for the 3800 m. Since the unobserved interval occurred in
329 winter, the missing sampling period was filled using an average flux value of the winter
330 cups (first and last trap bottles). In the case of the SAM trap, the number of samples
331 available for CaCO_3 and calcareous nannoplankton analyses was different, covering a
332 period of 313 and 191 days respectively. Since gaps were quasi-equally distributed along
333 the time series, annual fluxes were estimated by filling the gaps in the record with average
334 fluxes calculated from the available data. The estimated range of the annual contribution
335 of coccolithophores to total CaCO_3 export at the SOTS and SAM traps was calculated by
336 multiplying the coccolith flux of each species in each sampling interval by its average
337 coccolith weight values obtained with the birefringence and morphometric techniques.

338 **2.8 Remotely sensed chlorophyll-*a* and PIC concentrations**

339 Weekly Chlorophyll-*a* and PIC concentrations for the sampling intervals at the
340 SOTS and SAM sites were derived from Giovanni online data system, developed and
341 maintained by the NASA Goddard Earth Sciences Data Active Archive Center (Acker
342 and Leptoukh, 2007). Each value is a weekly value is produced by computing spatial
343 averages within the area 48.5-45.5°S and 130-150°E for the SOTS site and 47-45° S and
344 171°E-179°W for the SAM site (Fig. 5).

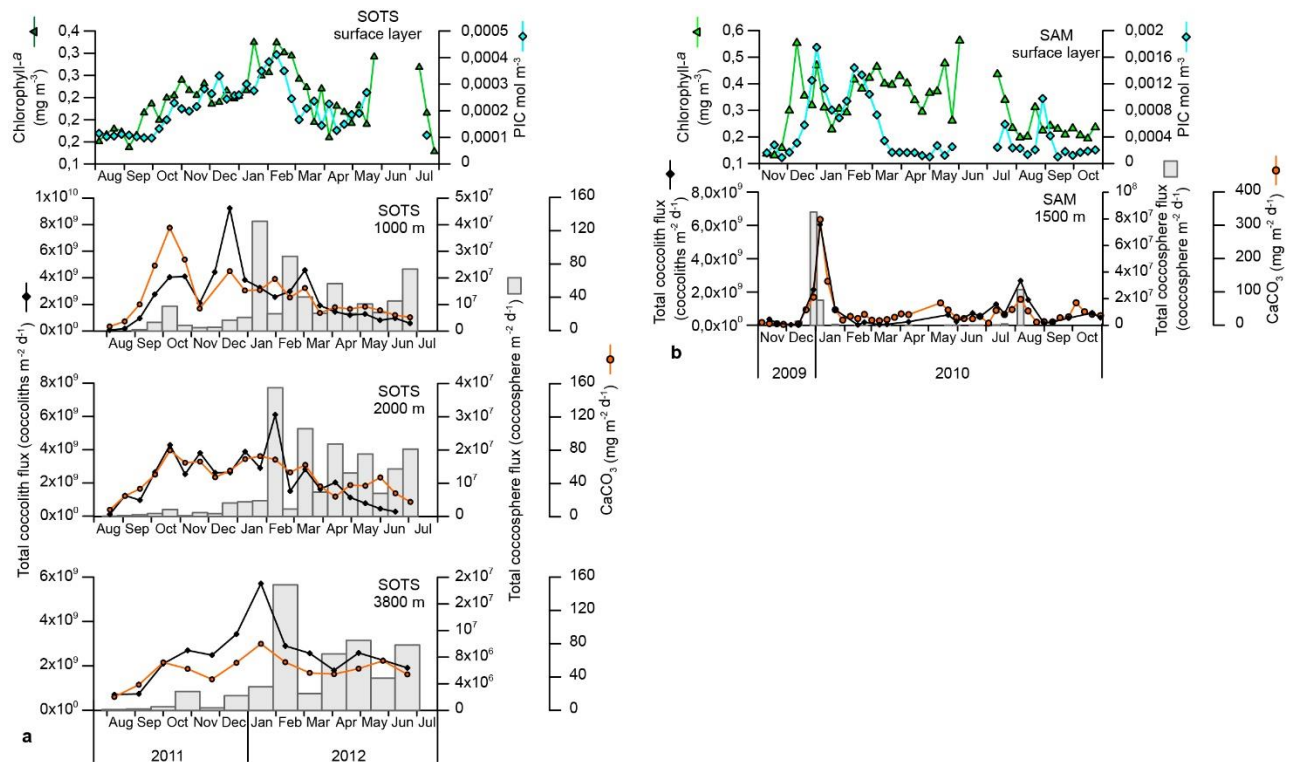
345

346 **3. RESULTS**

347 **3.1 Magnitude and seasonality of coccolithophore and CaCO_3 fluxes**

348 Annualized coccolith fluxes were similar at the SOTS three trap depths, with 8.6,
349 7.3 and 8.6×10^{11} liths $\text{m}^{-2} \text{yr}^{-1}$ at 1000, 2000 and 3800 m respectively, and about three
350 times larger than those of the SAM site (3.0×10^{11} liths $\text{m}^{-2} \text{yr}^{-1}$). The contribution of
351 intact coccospheres to the total coccolith export was low at both sites, with annual
352 coccosphere fluxes two orders of magnitude lower than coccolith fluxes at SOTS (3.5,
353 3.3 and 1.8×10^9 coccospheres $\text{m}^{-2} \text{yr}^{-1}$ at 1000, 2000 and 3800 m, respectively) and SAM
354 (2.2×10^9 coccospheres $\text{m}^{-2} \text{yr}^{-1}$). Annualized CaCO_3 export was similar at both sites with
355 14.6, 16.2 and $17.1 \text{ g m}^{-2} \text{yr}^{-1}$ at 1000, 2000 and 3800 m at the SOTS site and 13.9 g m^{-2}
356 yr^{-1} at the SAM sediment trap (1500 m).

357 Both coccolith and coccosphere fluxes displayed a marked seasonality that
358 followed the general trend of algal biomass accumulation in the surface waters at the
359 SOTS and SAM sites (Fig. 2). Coccolith fluxes at 1000 m started to increase in early
360 October and remained above the threshold of 1×10^9 coccoliths $\text{m}^2 \text{d}^{-1}$ until mid-April
361 (Fig. 2). Three maxima were recorded during the period of high coccolith export:
362 October-early November 2011 (4×10^9 coccoliths $\text{m}^2 \text{d}^{-1}$), late December 2011 (9×10^9
363 coccoliths $\text{m}^2 \text{d}^{-1}$) and March 2012 (4×10^9 coccoliths $\text{m}^2 \text{d}^{-1}$). Coccolith fluxes of the
364 main coccolithophore species generally followed the similar seasonal pattern to that of
365 the total coccolith flux (Supplementary figure 1) and are not discussed further.
366 Coccolithophore fluxes registered by the 2000 and 3800 m sediment traps followed a
367 generally similar seasonal pattern to those of the shallower trap at the SOTS site (Fig. 2).
368 At SAM, coccolith fluxes exhibited a strong seasonality with peak fluxes in early January
369 2010 (up to 6×10^9 coccoliths $\text{m}^2 \text{d}^{-1}$) and a secondary peak in August 2010 (3×10^9
370 coccoliths $\text{m}^2 \text{d}^{-1}$). Coccosphere fluxes at both sites displayed maximum fluxes during the
371 austral summer and minima during winter; however maximum coccosphere export peaks
372 did not always match those of coccolith export (Fig. 2). The seasonality of total CaCO_3
373 followed a similar pattern to coccolith fluxes with peak values in the spring-summer and
374 minima during winter at both study sites.



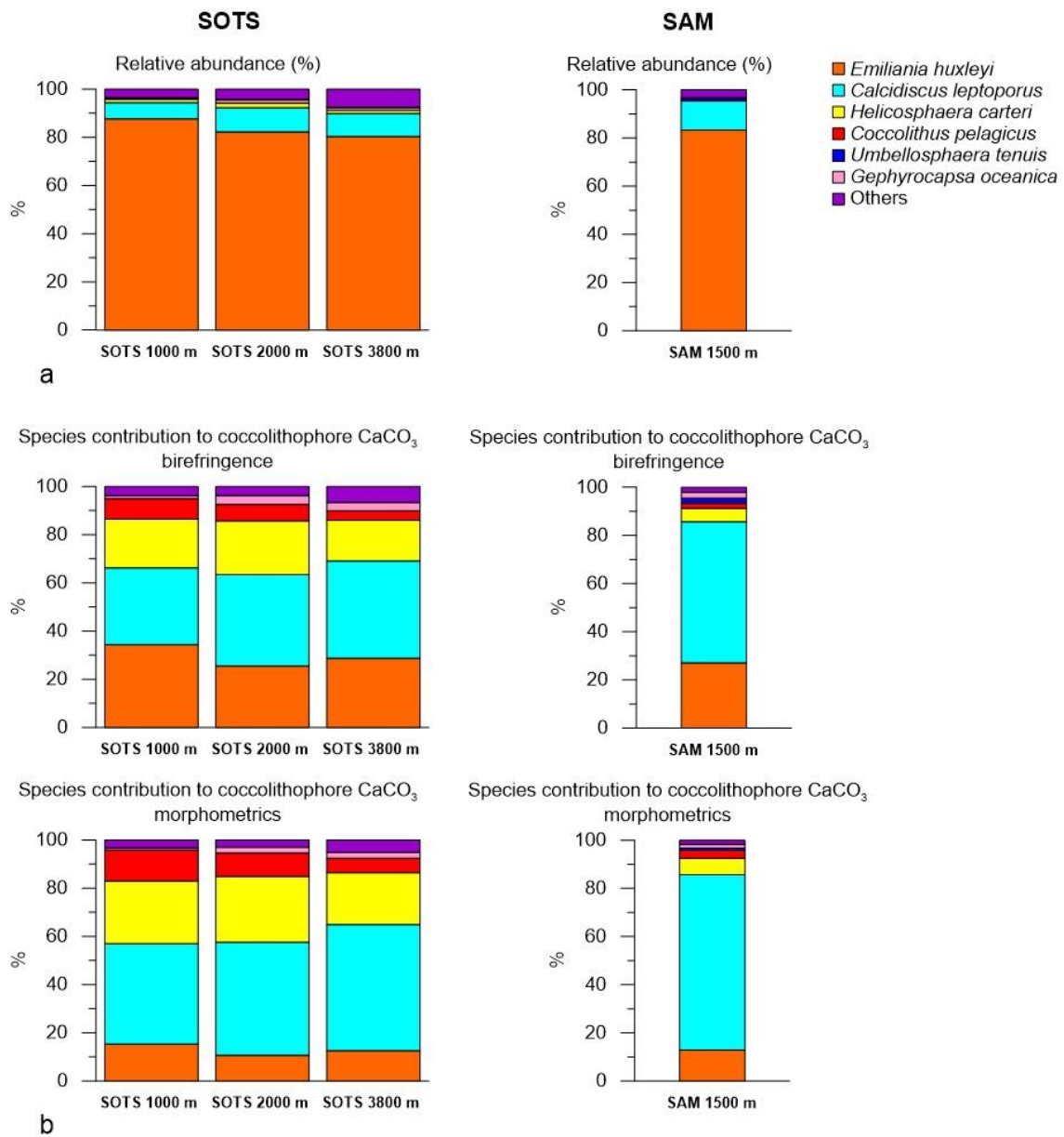
375

376 **Figure 2: Ocean-colour** satellite-derived chlorophyll-a and Particulate Inorganic Carbon
 377 (PIC) concentration in the surface layer and total CaCO₃, coccolith and coccospere
 378 fluxes registered by the sediment traps at the SOTS (a) and SAM (b) sites.

379 **3.2. Coccolithophore assemblage composition**

380 Coccolith sinking assemblages were overwhelmingly dominated by *Emiliana*
 381 *huxleyi* for all sediment trap records analysed (Fig. 3a). At the SOTS site, the annualized
 382 flux-weighted relative contribution of *E. huxleyi* decreased slightly with depth,
 383 comprising 88% of the total coccolithophore assemblage at 1000 m, 82% at 2000 m and
 384 80% at 3800 m. Secondary components of the coccolith sinking assemblage were
 385 *Calcidiscus leptoporus (sensu lato)* (6.8, 10.1 and 9.6% at 1000, 2000 and 3900 m,
 386 respectively), *Helicosphaera carteri* (1.4, 2 and 1.3%) and small *Gephyrocapsa* spp. (<
 387 3 μm) (1.4, 1.5 and 4.7%). Background concentrations (≤ 1%) of *Calciosolenia* spp.,
 388 *Coccolithus pelagicus*, *Gephyrocapsa muelleriae*, *Gephyrocapsa oceanica*,
 389 *Gephyrocapsa* spp. (> 3 μm), *Syracosphaera pulchra*, *Syracosphaera* spp.,
 390 *Umbellosphaera tenuis (sensu lato)*, and *Umbilicosphaera sibogae* were also registered.
 391 At the SAM site, *E. huxleyi* accounted for 83% of the annualized coccolith flux, with
 392 subordinate contributions of *C. leptoporus* (12.2%) and *Gephyrocapsa* spp. (< 3 μm)
 393 (1.5%). Background concentrations (< 1%) of *Calciosolenia* spp., *Coccolithus pelagicus*,

394 *G. oceanica*, *Gephyrocapsa muellerae*, *Gephyrocapsa* spp. (> 3 μm), *H. carteri*,
 395 *Syracosphaera pulchra*, *Syracosphaera* spp., *U. sibogae* and *U. tenuis* were observed.



396 **Figure 3: a.** Annualized integrated relative abundance of the most important
 397 coccolithophore species in the SOTS and SAM sediment trap records. **b.** Fractional
 398 contribution of coccolithophore species to total coccolithophore CaCO₃ export in the
 399 SOTS and SAM sediment traps.
 400

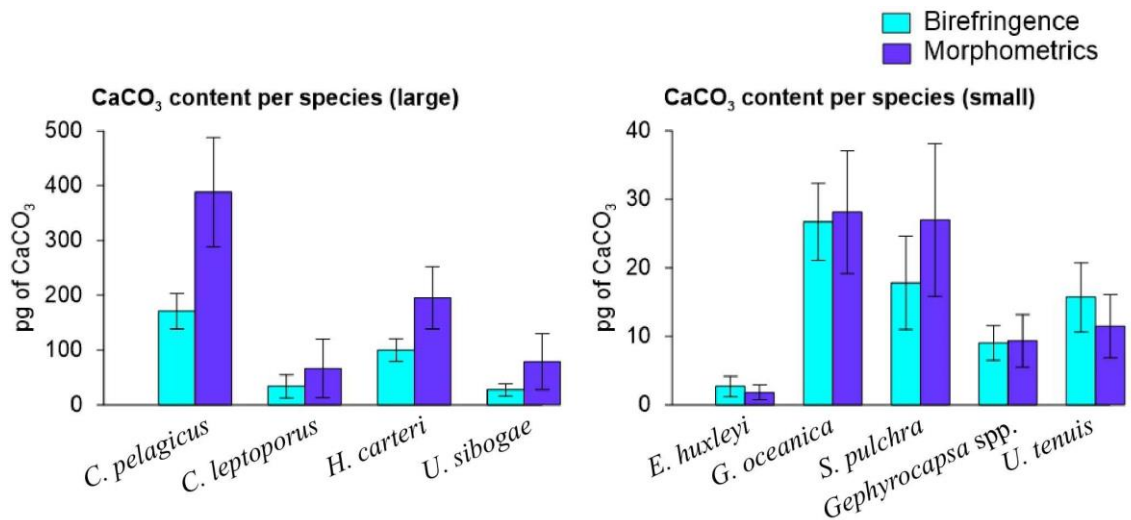
401 3.3 Calcite content per species

402 Coccolith length and mass for all species measured using birefringence and
 403 morphometric techniques are provided in Table 1. Overall, the average coccolith mass
 404 estimates for the coccolithophore species at SOTS and SAM sites using both approaches

405 are within the range of values in the published literature. The Noelaerhabdaceae family
 406 members, *G. oceanica* and *Gephyrocapsa* spp., display almost identical mass values with
 407 both approaches (Fig. 4). In contrast, substantial discrepancies are identifiable for *C.*
 408 *pelagicus*, *C. leptoporus*, *H. carteri* and *U. sibogae*, for which coccolith mass estimates
 409 are about two-fold greater using morphometrics than with the birefringence approach.
 410 The range of annual contributions of coccolithophores to carbonate is illustrated in Figure
 411 5.

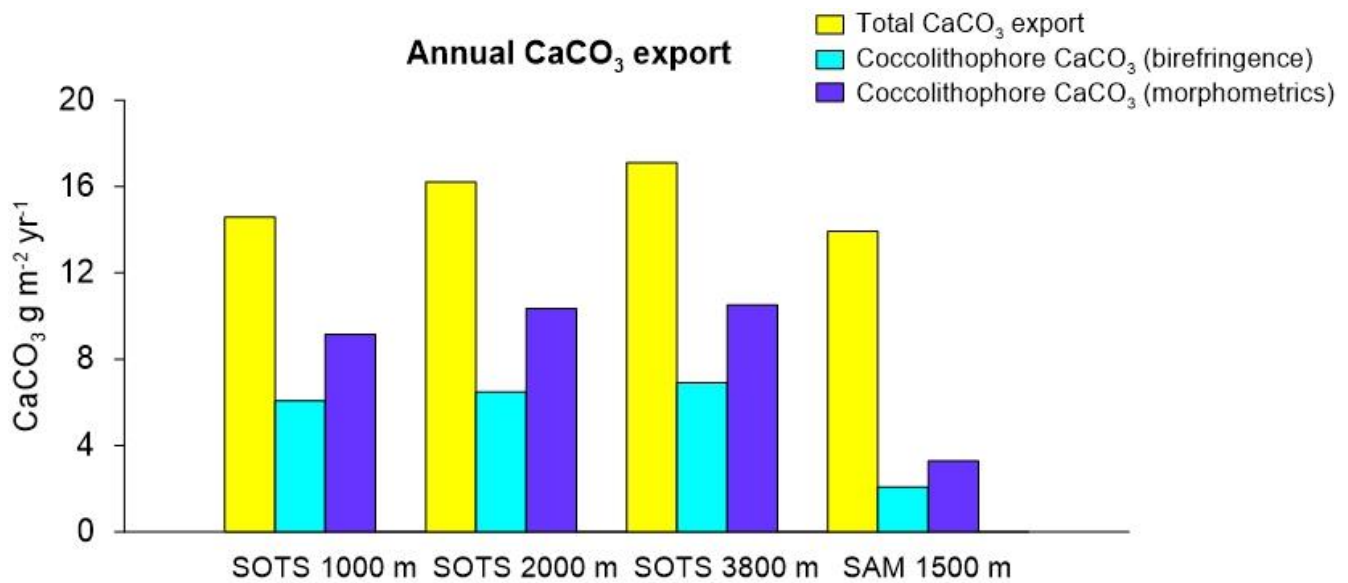
Species and morphotypes	Type of measurement	n	Length (µm)		Mass CaCO ₃ (pg)		k _s	Crystal units types	References
			Average	SD	Average	SD			
<i>Calcidiscus leptoporus</i>	Birefringence	210	6.39	1.49	33.65	21.11	-	V and R	
	Morphometrics	210	6.39	1.49	66.23	53.28	0.080		1
	Literature estimates	-	4.3-9.6		22.6-125.2		0.061-0.105		1,2
<i>Coccolithus pelagicus</i>	Birefringence	54	13.28	1.14	170.90	32.33	-	V and R	
	Morphometrics	54	13.28	1.14	387.96	99.64	0.060		1
	Literature estimates	-	8.5-13.5		99.5-398.6		0.051 - 0.060		1,2,3
<i>Emiliana huxleyi</i>	Birefringence	12842	2.78	0.57	2.64	1.43	-	R	
	Morphometrics	12842	2.78	0.57	0.99-2.64 (1.81)*	0.60-1.60	0.015-0.04 (0.0275)*	(V-unit vestigial)	
<i>E. huxleyi</i> type A	Literature estimates	-	3-4		1.50 - 3.50		0.02		1,4,5
<i>E. huxleyi</i> type A/o/c	Literature estimates	-	3.5		4.6		0.04		1
<i>E. huxleyi</i> type B/C	Literature estimates	-	1.8-5.5		0.3-3.5		0.015		5,6,7
<i>E. huxleyi</i> type B	Literature estimates	-	3.5-5		2.30 - 6.81		0.02		1,5
<i>Gephyrocapsa oceanica</i>	Birefringence	51	5.87	0.62	26.70	5.64	-	R	
	Morphometrics	51	5.87	0.62	28.14	8.97	0.050	(V-unit vestigial)	
	Literature estimates	-	5-5.35		16.9-25.7		0.050-0.062		1,2
<i>Gephyrocapsa</i> spp.	Birefringence	10	4.03	0.59	9.00	2.51	-	R	
	Morphometrics	10	4.03	0.59	9.33	3.84	0.050	(V-unit vestigial)	1
	Literature estimates	-	-	-	-		-		
<i>Helicosphaera carteri</i>	Birefringence	64	11.20	1.12	100.10	20.34	-	V and R	
	Morphometrics	64	11.20	1.12	194.95	56.45	0.050		1
	Literature estimates	-	9.1-10		135-142.8		0.050-0.070		1,2
<i>Syracosphaera pulchra</i>	Birefringence	81	6.77	1.09	17.77	6.80	-	V, R and T	
	Morphometrics	81	6.77	1.09	26.94	11.16	0.030		1
	Literature estimates	-	2.7-6		13.5-16.5		0.027-0.083		1,2,4
<i>Umbellosphaera tenuis</i>	Birefringence	54	6.42	0.99	15.69	5.02	-	R	
	Morphometrics	54	6.42	0.99	11.45	4.61	0.015		1
	Literature estimates	-	5-6		8.7-23.9		0.015-0.071		1,2
<i>Umbilicosphaera sibogae</i>	Birefringence	6	7.76	1.81	27.14	11.07	-	V and R	
	Morphometrics	6	7.76	1.81	78.93	51.38	0.055		1
	Literature estimates	-	4.1-6		16-35		0.055-0.086		1,2

412 **Table 1:** Coccolith mass estimates of the main coccolithophore species found at the SOTS
 413 and SAM sites using birefringence (C-Calcita) and morphometrics. Additionally, length
 414 and mass estimates from the literature are also listed for most species. References: (1)
 415 Young and Ziveri (2000), (2) Beaufort and Heussner (1999), (3) Samtleben and Bickert
 416 (1990), (4) Poulton et al. (2010), (5) Poulton et al. (2011), (6) Holligan et al. (2010) and
 417 (7) Charalampopoulou et al. (2016). * coccolith mass range obtained applying the
 418 minimum and maximum k_s values for *E. huxleyi* found in the literature (i.e. 0.015 and
 419 0.04, respectively).



420

421 **Figure 4:** Average and standard deviation of the coccolith mass estimates of the most
 422 important coccolithophore species captured by the SOTS and SAM sediment traps using
 423 birefringence (C-Calcita) and morphometric approaches. For *E. huxleyi*, the
 424 morphometric-based coccolith mass estimate was calculated by applying a mean shape
 425 factor constant (k_s) value estimated from the range of all the morphotypes found at the
 426 SAZ (i.e. $k_s = 0.0275$, Table 1).



427

428 **Figure 5:** Total annual CaCO₃ export (chemically determined) and fractional
 429 contribution of coccolithophores to CaCO₃ estimated using birefringence (C-Calcita)
 430 and morphometric approaches for the SOTS and SAM sites.

431 4. Discussion

432 4.1 Coccolithophore phenology in the SAZ: satellite versus sediment trap records

433 Total coccolith flux seasonality at the SOTS site shows good congruence with satellite-
434 derived PIC in the surface layer, with both parameters suggesting enhanced
435 coccolithophore productivity between October and March (austral mid-spring to early
436 autumn; Fig. 2a). Interestingly, substantial coccosphere export ($> 1 \times 10^7$ coccospheres
437 $\text{m}^2 \text{d}^{-1}$) does not occur until January indicating that coccolith and coccosphere export are
438 not tightly coupled in the subantarctic waters south of Australia. Two different processes
439 could be invoked to explain the mismatch between coccolith and coccosphere fluxes at
440 this site. Firstly, *E. huxleyi*, the dominant coccolithophore species in the Southern Ocean,
441 is able to produce coccoliths rapidly (up to three coccoliths per hour; Paasche, 1962;
442 Balch et al., 1996) and shed the excess of coccoliths into the surrounding water under
443 certain environmental conditions (Paasche, 2002). Although the coccolith shedding rate
444 of *E. huxleyi* increases linearly with cellular growth rate (Fritz and Balch, 1996; Fritz,
445 1999), the tiny size and low weight of detached coccoliths allow them to remain in the
446 upper water column long after cell numbers have begun to decline. It follows that high
447 concentrations of detached coccoliths do not necessary imply a proportional abundance
448 of coccospheres in the surface layer (Tyrrell and Merico, 2004; Poulton et al., 2013) or in
449 the traps. Additionally, a substantial fraction of the coccospheres produced in the surface
450 layer may experience substantial mechanical breakage by zooplankton before reaching
451 the trap depths. Indeed, microzooplankton grazing pressure can remove up to 82% of
452 primary production in mid-summer in the subantarctic waters south of Tasmania
453 (Ebersbach et al., 2011) and about 60% of the daily coccolithophore growth in the North
454 Atlantic (Mayers et al., 2019), therefore suggesting a strong top-down control on
455 coccolithophore populations. Additionally, a polyacrylamide gel sediment traps study in
456 the subantarctic waters south of Tasmania by Ebersbach et al. (2011) revealed that most
457 of the particles exported out the mixed layer during the productive period occur in the
458 form of faecal aggregates. Therefore, it is highly likely that: (i) the intensity of
459 coccosphere export registered by the traps is influenced by grazing pressure in the surface
460 layer, and (ii) that the impact of grazing on coccolithophores varies throughout the year
461 (Calbet et al., 2008; Lawrence and Menden-Deuer, 2012; Quéguiner, 2013).

462 In contrast, seasonal variations in satellite-derived PIC concentration and
463 coccolith fluxes at SAM show some discrepancies not observed at SOTS. While
464 maximum PIC concentrations in the surface layer and coccolith and coccosphere fluxes
465 co-occur in December and January (austral early to mid-summer), satellite-derived PIC
466 suggests a secondary maximum in February-early-March not recorded by the trap (Fig.

467 2b). One possibility is that the satellite secondary maximum is not coccoliths. The higher
468 chlorophyll-a levels at the SAM site (Fig. 2) suggests that other phytoplankton groups,
469 such as diatoms, are more abundant than in the subantarctic waters south of Tasmania.
470 Empty and broken diatom valves have been suggested to display similar spectral
471 characteristics than those of coccolithophore blooms (Broerse et al., 2003; Tyrrell and
472 Merico, 2004; Winter et al., 2014). Therefore, the second peak in satellite-derived PIC
473 could have been caused by a senescent diatom bloom. This hypothesis is likely since
474 diatom blooms in the SAZ are known to develop early in the productive season (Rigual-
475 Hernández et al., 2015b) and rapidly decay following the depletion of silicate and/or iron
476 stocks in the surface layer (Lannuzel et al., 2011). However, no secondary late summer
477 maximum was observed in biogenic silica fluxes in the SAM. Another possible
478 explanation is a contribution to the satellite record from lithogenic material or storm-
479 induced microbubble injection (Zhang et al., 2002). Fully resolving causes of mismatches
480 between *in-situ* and satellite PIC estimates is not achievable for the SAM site (nor more
481 broadly for the Southern Ocean; Trull et al., 2018).

482 A second difference between the SAM and SOTS sites is that maximum annual
483 coccosphere export occurred one week earlier than maximum coccolith fluxes at SAM,
484 (Fig. 2). The different seasonalities between the sites suggest that different export
485 mechanisms may operate. The formation of rapidly sinking algal aggregates by diatoms
486 is known to scavenge particles they have collided with and increase particle sinking
487 (Alldredge and McGillivray, 1991; Passow and De La Rocha, 2006), thus the formation
488 of such rapid-sinking aggregates could potentially facilitate the preservation of
489 coccospheres early in the productive season at the SAM site. However, the lack of
490 accompanying *in situ* information on plankton community structure in the study region
491 precludes the assessment of these hypotheses.

492 Despite the uncertainties involved in our interpretations, the overall picture that
493 emerges from our comparison of satellite and sediment trap flux data is that the duration
494 of the coccolithophore bloom based on ocean-colour-based PIC concentrations most
495 likely provides an over-estimation of the coccolithophore productive season. Our
496 observations motivate caution in describing coccolithophore phenology solely based on
497 satellite-derived PIC concentrations (e.g. Hopkins et al., 2015).

498

499 **4.2 Magnitude and composition of subantarctic coccolithophore assemblages**

500 Annual coccolith export across the major zonal systems of the Australian sector
501 of the Southern Ocean exhibits a clear latitudinal gradient, with maximum fluxes at the
502 SAZ (8.6×10^{11} liths $m^{-2} yr^{-1}$) and eight-fold lower fluxes in the polar waters of the AZ
503 (1.0×10^{11} liths $m^{-2} yr^{-1}$; Rigual Hernández et al., 2018). Coccolithophore species
504 occurrence documented by our subantarctic sediments traps are consistent with previous
505 reports on coccolithophore assemblage compositions in the surface layer (Findlay and
506 Giraudeau, 2000; Saavedra-Pellitero et al., 2014; Malinverno et al., 2015; Chang and
507 Northcote, 2016) and sediments (Findlay and Giraudeau, 2000; Saavedra-Pellitero and
508 Baumann, 2015) and are more diverse than those found in the AZ (Rigual Hernández et
509 al., 2018). The southward decline in coccolithophore abundance and diversity is most
510 likely due to the decrease in sea-surface temperature (SST) and light availability moving
511 poleward (Charalampopoulou et al., 2016; Trull et al., 2018). In particular, the close
512 relationship between temperature and growth rates has been demonstrated in a range of
513 coccolithophore species and strains (Buitenhuis et al., 2008), and seems to be a critical,
514 if not the most important, control on the biogeographical distribution of coccolithophore
515 species in the Southern Ocean (Trull et al., 2018). This pronounced latitudinal change in
516 coccolithophore assemblage composition contrasts with the little longitudinal variability
517 between the subantarctic SOTS and SAM sites (Fig. 3). These observations underscore
518 the role of circumpolar fronts as natural physical barriers for plankton species distribution
519 in the Southern Ocean (Medlin et al., 1994; Boyd, 2002; Cook et al., 2013).

520 Notably, the rare occurrence of the cold-water species *Coccolithus pelagicus* at
521 the SOTS and SAM sites contrasts with the high contribution of *C. pelagicus* to the living
522 coccolithophore communities in the subpolar and polar waters of the North Atlantic and
523 North Pacific oceans, where it is often the second most abundant species after *E. huxleyi*
524 (McIntyre and Bé, 1967; Baumann et al., 2000; Broerse et al., 2000a; Broerse et al.,
525 2000b; Ziveri et al., 2000). This important difference in species composition between
526 Northern and Southern hemisphere subpolar ecosystems could have important
527 implications in the calibration of the satellite PIC signal in the Southern Ocean. Previous
528 research in the Southern Ocean comparing satellite and shipboard observations identified
529 a substantial over-estimation of coccolithophore PIC in the Southern Ocean waters by
530 satellite ocean-colour-based PIC algorithms (Holligan et al., 2010; Trull et al., 2018).
531 Since satellite reflectance observations are mainly calibrated against Northern
532 Hemisphere PIC results (Balch et al., 2011; Balch et al., 2016), the lower the calcite
533 content of dominant *E. huxleyi* morphotypes (B/C) in the Southern Ocean compared to

534 their northern hemispheric counterparts has been suggested as a possible factor causing
535 the over-estimation of PIC concentrations in the Southern Ocean. Following this
536 reasoning, we speculate that differences in other components of the coccolithophore
537 assemblages, and particularly, differences in *C. pelagicus* numbers, could contribute to
538 the over-estimation of PIC concentrations by the satellite PIC algorithm in the Southern
539 Ocean. Indeed, the scaling of reflectance (in satellite images) to PIC (in ocean) is very
540 dependent on coccolith area:mass ratios (Gordon and Du, 2001; Balch et al., 2005a).
541 *Coccolithus pelagicus* has remarkably heavier and thicker coccoliths (100-400 pg per
542 coccolith; Table 1) than *E. huxleyi* (~3 pg per coccolith), i.e. about 100 times heavier.
543 However, the average coccolith area of *C. pelagicus* is only about ten times greater than
544 that of *E. huxleyi*. Thus, this lack of proportional relationship between area and mass
545 between these species should be taken into consideration when calibrating the satellite
546 signals of coccolithophore-related PIC in the Southern Ocean. However, it should be
547 noted that this is only one possible factor contributing to the overestimation of PIC
548 concentrations in Southern Ocean waters. Other factors such as the presence of
549 microbubbles -- that are a source of enhanced reflectance -- must also play an important
550 role (Balch et al., 2011).

551

552 **4.3 Coccolith calcite content of subantarctic coccolithophore species**

553 Multiple methodological biases associated with each of the methods used for
554 estimating coccolith calcite content (i.e. birefringence, morphometrics) could be invoked
555 to explain the different estimates observed for some of the species (see Young and Ziveri,
556 2000; Fuertes et al., 2014 and references therein). However, the fact that these
557 discrepancies vary greatly across species suggests that the composition of the crystal-
558 units of the coccoliths could be the most important factor causing these differences. All
559 the heterococcoliths of the species analysed are mainly composed of either V- or R-
560 calcite crystal units or a combination of both (Young et al., 2003; Table 1). R units are
561 characterized by sub-radial c-axes that are reasonably well measured by the birefringence
562 technique, but, the almost vertical optical axes of the V units (Young, 1992; Young et al.,
563 1999) make the same thickness less birefringent (Fuertes et al., 2014). Thus, it is likely
564 that differences in the birefringence properties of the R and V units could be responsible
565 for the different estimates provided by the two approaches. This is supported by our
566 results which show coccolith mass estimates of those species composed of R units, such

567 as *G. oceanica* and *Gephyrocapsa* spp. exhibit almost identical values with both
568 techniques (Table 1). In contrast, those species with coccoliths composed by a
569 combination of R and V units, such as *C. pelagicus*, *C. leptoporus*, *H. carteri* and *U.*
570 *sibogae*, display divergent mass estimates between approaches. The case of *E. huxleyi* is
571 more complex due to the large intraspecific genetic variability that results in substantial
572 differences in the profile and degree of calcification between specimens (Young and
573 Ziveri, 2000). Our birefringence mass estimate for *E. huxleyi* (2.67 ± 1.49 pg) is less than
574 one picogram lower than the mean range value calculated with the morphometric
575 technique (i.e. 1.81 ± 1.10 pg with an average k_s value of all the morphotypes found at
576 the SAZ, i.e. $k_s = 0.0275$), but identical to the maximum (2.64 ± 1.60 pg; using $k_s = 0.04$).
577 These results suggest a reasonably good consistency between techniques for *E. huxleyi*.

578 Taking into consideration all the above, it is likely that the coccolith mass of some
579 species is underestimated by the birefringence technique, and therefore, the fractional
580 contribution of coccolithophores to total PIC using this approach should be taken as a
581 conservative estimate. Since both methods for estimating calcite content have inherent
582 uncertainties, the range of values provided by both techniques is used here as an
583 approximation of the fractional contribution of coccolithophores to total annual CaCO_3
584 export to the deep sea in the Australian and New Zealand sectors of the SAZ.

585 **4.4 Contribution of coccolithophores to carbonate export in the Australian-New** 586 **Zealand sectors of the Southern Ocean**

587 The magnitude of the total PIC export in the subantarctic waters was similar
588 between the SOTS and SAM sites (range $14\text{-}17$ g m^{-2} yr^{-1}), and thus slightly above the
589 global average (11 g m^{-2} yr^{-1} ; Honjo et al., 2008). Our estimates indicate that
590 coccolithophores are major contributors to CaCO_3 export in the Australian and New
591 Zealand waters of the SAZ, accounting for 40-60% and 15-25% of the annual CaCO_3
592 export, respectively (Fig. 5). Heterotrophic calcifiers, mainly planktonic foraminifera
593 (Salter et al., 2014), must therefore account for the remainder of the annual CaCO_3 export
594 at both sites. Previous work on foraminifera fluxes in our study regions allows an
595 approximate estimate of the contribution of foraminifera to total CaCO_3 flux that can be
596 used to assess the validity of our estimates. Combining counts of foraminifera
597 shells (King and Howard, 2003) with estimates of their average shell weights ($20\text{-}40$ μg
598 per shell depending on size; Moy et al., 2009) suggests contributions of 1/3 to 2/3 of
599 planktonic foraminifera to the total CaCO_3 flux in the Australian SAZ (Trull et al., 2018).

600 In the subantarctic waters south of New Zealand, Northcote and Neil (2005) estimated
601 that planktonic foraminifera accounted for about 78-97% of the total CaCO₃. Thus,
602 estimations of the contribution of heterotrophic calcifiers to total carbonate in both study
603 regions are in reasonable agreement with our coccolithophore CaCO₃ estimates at both
604 sites. The lower contribution of coccolithophores to CaCO₃ export at the SAM site in
605 comparison with that of SOTS may be explained by differences in the ecosystem structure
606 between sites. Algal biomass accumulation in the surface waters of the SAM region
607 (average chlorophyll-*a* concentration between 2002 and 2018 is 0.31 mg m⁻³) is
608 substantially higher than that at SOTS (0.23 mg m⁻³). We speculate that the higher
609 abundance of non-calcareous phytoplankton (e.g. diatoms) in the subantarctic waters
610 south of New Zealand could simultaneously reduce coccolithophore biomass through
611 resource competition (Quéré et al., 2005; Sinha et al., 2010) while stimulating
612 foraminifera growth (Schiebel et al., 2017). The combination of both factors could be
613 responsible for the lower coccolithophore productivity at the SAM site despite similar
614 total CaCO₃ export. Assuming that both the SOTS and SAM sites can be considered
615 representative of a broad longitudinal swath of the SAZ south of Australia and New
616 Zealand (ca. 1% of areal extent of the global ocean), the coccolithophore CaCO₃ export
617 in these two regions together account for approximately 0.4 Tmol C_{inorg} yr⁻¹. This value
618 represents approximately 1% of the global annual PIC export to the deep ocean (Honjo et
619 al., 2008) and underscores the notion that the high nutrient low-chlorophyll waters of the
620 circumpolar SAZ should not be taken as indicative of low biological activity or export.

621 Our results indicate that although *E. huxleyi* overwhelmingly dominates the
622 coccolithophore sinking assemblages at both study sites, other species with lower relative
623 contribution but substantially heavier coccoliths are more important contributors to the
624 annual coccolithophore CaCO₃ export budget (Fig. 3). Particularly relevant is the case of
625 *C. leptoporus* that despite its relatively low abundance (~ 10% of the annual assemblage
626 at both sites; Fig. 3), it accounts for between 30-50% and 60-70% of the annual
627 coccolithophore-CaCO₃ export at the SOTS and SAM sites, respectively (Fig. 3).
628 Similarly, other species with heavy coccoliths, such as *H. carteri* and *C. pelagicus*, are
629 important contributors to the annual coccolithophore PIC export to the deep sea (up to
630 ~30% and ~10% of the annual coccolithophore PIC, respectively) despite their low annual
631 relative abundance (<2% at both sites) (Fig. 3). These results serve as an important
632 reminder that it is often not the most abundant species, but rather the largest

633 coccolithophore species that account for the greatest contribution to coccolithophore
634 CaCO₃ production and export (Young and Ziveri, 2000; Baumann et al., 2004; Daniels et
635 al., 2016).

636 The important contribution made by the coccolithophore community in setting the
637 magnitude of carbonate production and export to the deep sea is evidenced when we
638 compare the coccolith and total CaCO₃ fluxes of the SOTS sediment trap with those
639 deployed in the AZ along the 140°E meridian (Fig. 1). Although both total and
640 coccolithophore CaCO₃ export decrease with increasing latitude these changes are largely
641 uneven. While total CaCO₃ decreases two-fold from the SAZ to the AZ, coccolithophore
642 CaCO₃ export decreases 28-fold (Supplement Figure 2). This lack of proportional
643 latitudinal change can be attributed to two main factors. First, subantarctic
644 coccolithophore populations are diverse and relatively rich in species with large and
645 heavy coccoliths such as *C. leptoporus* or *H. carteri* that account for a large fraction of
646 the annual carbonate production and export. South of the PF, assemblages become
647 monospecific, or nearly monospecific, dominated by the small and relatively lightly
648 calcified *E. huxleyi*. Second, latitudinal variations in the abundance of heterotrophic
649 calcifiers (mainly foraminifera but also pteropods) must play a major role in modulating
650 the observed variations in CaCO₃ export. In particular, our data suggests that the
651 fractional contribution of heterotrophic calcifiers to CaCO₃ production increases from
652 ~40-60 % in the Australian SAZ to up to 95% in the AZ (Rigual Hernández et al., 2018).
653 This pattern is consistent with previous shipboard and sediment trap studies that reported
654 higher abundances of planktonic foraminifera at the PFZ and AZ compared to that of the
655 SAZ in the Australian sector (King and Howard, 2003; Trull et al., 2018). Controls on the
656 biogeographic distribution of foraminifera species are complex and beyond the scope of
657 this paper, however, we provide a few observations. Both temperature and diet are critical
658 factors controlling the spatial distribution of planktonic foraminifera species. In
659 particular, the lower temperatures south of the SAF seem to favour the development of
660 *Neogloboquadrina pachyderma* sin. and *Turborotalita quinqueloba* as indicated by the
661 high abundance of these species in the PFZ (> 80% of the annual integrated flux for both
662 species together; King and Howard, 2003). Additionally, the dramatically different algal
663 communities dwelling in each zonal system may also play a role in planktonic
664 foraminifera species distributions. In particular, diatoms can account for a major part of
665 the diet of some foraminifera species, including *N. pachyderma* (Schiebel and Hemleben,

666 2017). Therefore, it is likely that the preferential grazing on diatoms of some foraminifera
667 species may play an important role in the increase of foraminifera CaCO₃ production
668 moving poleward.

669

670 **4.5 Future predictions of coccolithophore community response to environmental** 671 **change in the subantarctic zone**

672 The response of *E. huxleyi* to environmental change has been extensively studied
673 in laboratory experiments (Meyer and Riebesell, 2015; Müller et al., 2015; Feng et al.,
674 2017) and the available information is sufficient to propose possible changes of its niche
675 and calcification in the Southern Ocean, as discussed in detail in Trull et al. (2018) and
676 Krumhardt et al. (2017). Due to the ubiquity and abundance of *E. huxleyi*, the
677 ecophysiology of this species is often regarded as typical of all coccolithophores.
678 However, *E. huxleyi* is rather different from most other coccolithophore species in that its
679 physiological adaptations place it in the upper limit of the *r-K* ecological gradient of these
680 organisms (i.e. an opportunistic species), while most of the other species are located at
681 the opposite end of the spectrum (i.e. conservative or K-selected species) (Probert and
682 Houdan, 2004). Our results demonstrate that *E. huxleyi* plays an important, but not
683 dominant role in CaCO₃ export, with other species such as *C. leptoporus*, *H. carteri* or *C.*
684 *pelagicus* making a larger contribution to the annual CaCO₃ export in the SAZ (Fig. 3).
685 Therefore, it is of critical importance to evaluate how these other biogeochemically
686 important coccolithophore species will respond to projected climate-induced changes in
687 the Southern Ocean. Here, we now assess the response of large coccolithophore species
688 to projected changes in temperature and carbonate chemistry, that have been highlighted
689 among the most important environmental stressors expected to impact Southern Ocean
690 coccolithophore physiological rates (Müller et al., 2015; Charalampopoulou et al., 2016;
691 Feng et al., 2017; Trull et al., 2018).

692 The Southern Ocean is warming rapidly (Gille, 2002; Böning et al., 2008), largely
693 due to the southward migration of the ACC fronts (Sokolov and Rintoul, 2009). Only
694 between 1992 and 2007 the position of Southern Ocean fronts shifted by approximately
695 60 km to the south (Sokolov and Rintoul, 2009) and this trend may continue throughout
696 the next century. Therefore, it is likely that any further southward migration of ACC
697 fronts will be coupled with an expansion of subantarctic coccolithophore species towards
698 higher latitudes. The poleward expansion of *E. huxleyi* geographic range has already been

699 suggested in the Southern Ocean (Cubillos et al., 2007; Winter et al., 2014;
700 Charalampopoulou et al., 2016) and it also appears to be occurring in the North Atlantic
701 (Rivero-Calle et al., 2015; Neukermans et al., 2018). Given the important contribution of
702 large subantarctic coccolithophore species to CaCO₃ export, the expansion of their
703 ecological niche could result in a substantial increase in CaCO₃ production and export in
704 the Southern Ocean. However, this may not be the future scenario for the SAZ southeast
705 on New Zealand, where bathymetry strongly controls the location of ocean fronts
706 (Fernandez et al., 2014; Chiswell et al., 2015). If the fronts are bathymetrically ‘locked’,
707 then the SAZ will not expand in areal extent, although the region is still predicted to
708 undergo significant physical, biogeochemical and biological changes (Law et al., 2017)
709 that will have likely flow-on effects on coccolithophore productivity and export
710 (Deppeler and Davidson, 2017).

711 The available carbonate chemistry manipulation experiments with *C. leptoporus*
712 have come to different conclusions. While some studies identified an increase in coccolith
713 malformations with increasing CO₂ concentrations (Langer et al., 2006; Langer and Bode,
714 2011; Diner et al., 2015), another study (Fiorini et al., 2011) reported no changes in the
715 calcification of *C. leptoporus* at elevated *p*CO₂. Interestingly, *C. leptoporus* did not
716 experience changes in its photosynthesis rates over the tested CO₂ range in any of the
717 aforementioned studies. The most likely explanation for the different results between the
718 studies is a strain-specific variable responses to changing carbonate chemistry (Diner et
719 al., 2015). Strain-specific variability in response to changing carbonate chemistry has
720 been previously reported in other coccolithophores, such as *E. huxleyi* (Langer et al.,
721 2009; Müller et al., 2015), and therefore it is likely that this also occurs in other species.
722 Given the fact that Southern Ocean fronts act as barriers for species distributions and gene
723 flows (Medlin et al., 1994; Patarnello et al., 1996; Thornhill et al., 2008; Cook et al.,
724 2013), it is possible that the subantarctic *C. leptoporus* populations exhibit a different
725 ecophysiology than those used in the above mentioned laboratory experiments. Prediction
726 of the responses of *H. carteri* and *C. pelagicus* is even more challenging due to the lack
727 of experiments testing the response of these species to changing seawater carbonate
728 chemistry. The only available insights in the response of one of these species to ocean
729 acidification are found in the fossil record. Both Gibbs et al. (2013) and O’Dea et al.
730 (2014) reconstructed the evolution of *C. pelagicus* populations during the Palaeocene-
731 Eocene Thermal Maximum (PETM), a period arguably regarded as the best geological
732 approximation of the present rapid rise in atmospheric CO₂ levels and temperatures.

733 These studies concluded that *C. pelagicus* most likely reduced its growth rates and
734 calcification during this period. This limited number of studies suggest that the ongoing
735 ocean acidification in the Southern Ocean could potentially have a negative impact on the
736 physiological rates of *C. leptoporus* and *C. pelagicus* while the effect on *H. carteri* is
737 unknown. Physiological response experiments (e.g. Müller et al., 2015) with Southern
738 Ocean strains of *C. leptoporus*, *H. carteri* and *C. pelagicus* are, therefore, urgently needed
739 to be able to quantify the effect of projected changes in oceanic conditions in the SAZ on
740 their physiological rates and consequent effects on carbon cycling in the Southern Ocean.

741 Our synthesis suggests opposing influence of environmental stressors on
742 subantarctic coccolithophore populations. Poleward migration of fronts will likely
743 increase coccolithophore CaCO₃ production in the Southern Ocean, while changes in
744 carbonate chemistry speciation will reduce growth rates of subantarctic coccolithophores.
745 It seems possible that coccolithophores will initially expand southward as waters warm
746 and fronts migrate, but then eventually diminish as acidification overwhelms those
747 changes.

748

749 **Acknowledgments**

750 This project has received funding from the European Union's Horizon 2020 research and
751 innovation programme under the Marie Skłodowska-Curie grant agreement number
752 748690 – SONAR-CO2 (ARH, JAF and FA). The SOTS mooring work was supported
753 by IMOS, the ACE CRC, and the Australian Marine National Facility. The work at SAM
754 was supported by funding provided by the New Zealand Ministry of Business, Innovation
755 and Employment and previous agencies, and most recently by NIWA's Strategic Science
756 Investment Fund. NIWA is acknowledged for providing capital grants for mooring
757 equipment purchases, and thanks to all the NIWA scientists, technicians and vessels staff,
758 who participated in the New Zealand biophysical moorings programme (2000-12).
759 Cathryn Wynn-Edwards (IMAS) provided support in sample splitting/processing and
760 laboratory analysis. Satellite Chlorophyll-*a* and PIC data sets were produced with the
761 Giovanni online data system, developed and maintained by the NASA GES DISC. We
762 thank Griet Neukermans and Alex Poulton for their constructive comments and
763 suggestions that helped improve and clarify this manuscript.

764

765 **Author contributions**

766 TWT, SDN, DMD and LN planned and performed the field experiment. ARH led the
767 coccolithophore study and performed sample processing and microscopy and image
768 analyses. AMB and ARH performed SEM analyses. ARH and SN performed numerical
769 analyses. ARH wrote the paper with feedback from all authors.

770 **Competing interests**

771 The authors declare no competing interests.

772

773 **Data Availability**

774 Morphometric data of major coccolithophore species generated during the current study are listed
775 in Table 1, while species relative abundance and species fluxes (plotted in Supplement Figure 1)
776 can be accessed in the following link:

777 https://data.aad.gov.au/metadata/records/Coccolithophore_Fluxes_SAZ_2009-2012.

778

779 **References**

- 780 Acker, J. G., and Leptoukh, G.: Online Analysis Enhances Use of NASA Earth Science Data, *Eos*,
781 *Transactions. AGU*, 88, 14-17, 2007.
- 782 Alldredge, A. L., and McGillivray, P.: The attachment probabilities of marine snow and their
783 implications for particle coagulation in the ocean, *Deep Sea Research Part A. Oceanographic*
784 *Research Papers*, 38, 431-443, [http://dx.doi.org/10.1016/0198-0149\(91\)90045-H](http://dx.doi.org/10.1016/0198-0149(91)90045-H), 1991.
- 785 Alvain, S., Le Quéré, C., Bopp, L., Racault, M.-F., Beaugrand, G., Dessailly, D., and Buitenhuis, E.
786 T.: Rapid climatic driven shifts of diatoms at high latitudes, *Remote Sensing of Environment*,
787 132, 195-201, <http://dx.doi.org/10.1016/j.rse.2013.01.014>, 2013.
- 788 Bach, L. T., Riebesell, U., Gutowska, M. A., Federwisch, L., and Schulz, K. G.: A unifying concept
789 of coccolithophore sensitivity to changing carbonate chemistry embedded in an ecological
790 framework, *Progress in Oceanography*, 135, 125-138,
791 <https://doi.org/10.1016/j.pocean.2015.04.012>, 2015.
- 792 Bairbakhish, A. N., Bollmann, J., Sprengel, C., and Thierstein, H. R.: Disintegration of aggregates
793 and coccospheres in sediment trap samples, *Marine Micropaleontology*, 37, 219-223,
794 [http://dx.doi.org/10.1016/S0377-8398\(99\)00019-5](http://dx.doi.org/10.1016/S0377-8398(99)00019-5), 1999.
- 795 Balch, W. M., Fritz, J., and Fernandez, E.: Decoupling of calcification and photosynthesis in the
796 coccolithophore *Emiliania huxleyi* under steady-state light-limited growth, *Marine Ecology*
797 *Progress Series*, 142, 87-97, 1996.
- 798 Balch, W. M., Gordon, H. R., Bowler, B. C., Drapeau, D. T., and Booth, E. S.: Calcium carbonate
799 measurements in the surface global ocean based on Moderate-Resolution Imaging
800 Spectroradiometer data, 110, doi:10.1029/2004JC002560, 2005a.
- 801 Balch, W. M., Gordon, H. R., Bowler, B. C., Drapeau, D. T., and Booth, E. S.: Calcium carbonate
802 measurements in the surface global ocean based on Moderate-Resolution Imaging
803 Spectroradiometer data, *Journal of Geophysical Research: Oceans*, 110, n/a-n/a,
804 10.1029/2004JC002560, 2005b.
- 805 Balch, W. M., Drapeau, D. T., Bowler, B. C., Lyczkowski, E., Booth, E. S., and Alley, D.: The
806 contribution of coccolithophores to the optical and inorganic carbon budgets during the
807 Southern Ocean Gas Exchange Experiment: New evidence in support of the "Great Calcite Belt"
808 hypothesis, *Journal of Geophysical Research: Oceans*, 116, n/a-n/a, 10.1029/2011JC006941,
809 2011.
- 810 Balch, W. M., Bates, N. R., Lam, P. J., Twining, B. S., Rosengard, S. Z., Bowler, B. C., Drapeau, D.
811 T., Garley, R., Lubelczyk, L. C., Mitchell, C., and Rauschenberg, S.: Factors regulating the Great
812 Calcite Belt in the Southern Ocean and its biogeochemical significance, *Global Biogeochemical*
813 *Cycles*, 30, 1124-1144, 10.1002/2016GB005414, 2016.
- 814 Baumann, K.-H., Böckel, B., and Frenz, M.: Coccolith contribution to South Atlantic carbonate
815 sedimentation, in: *Coccolithophores: From Molecular Processes to Global Impact*, edited by:

816 Thierstein, H. R., and Young, J. R., Springer Berlin Heidelberg, Berlin, Heidelberg, 367-402,
817 2004.

818 Baumann, K. H., Andruleit, H., and Samtleben, C.: Coccolithophores in the Nordic Seas:
819 comparison of living communities with surface sediment assemblages, Deep Sea Research Part
820 II: Topical Studies in Oceanography, 47, 1743-1772, [http://dx.doi.org/10.1016/S0967-](http://dx.doi.org/10.1016/S0967-0645(00)00005-9)
821 [0645\(00\)00005-9](http://dx.doi.org/10.1016/S0967-0645(00)00005-9), 2000.

822 Beaufort, L., and Heussner, S.: Coccolithophorids on the continental slope of the Bay of Biscay
823 – production, transport and contribution to mass fluxes, Deep Sea Research Part II: Topical
824 Studies in Oceanography, 46, 2147-2174, [https://doi.org/10.1016/S0967-0645\(99\)00058-2](https://doi.org/10.1016/S0967-0645(99)00058-2),
825 1999.

826 Beaufort, L.: Weight estimates of coccoliths using the optical properties (birefringence) of
827 calcite, Micropaleontology, 51, 289-297, 10.2113/gsmicropal.51.4.289, 2005.

828 Beaufort, L., Barbarin, N., and Gally, Y.: Optical measurements to determine the thickness of
829 calcite crystals and the mass of thin carbonate particles such as coccoliths, Nature Protocols, 9,
830 633, 10.1038/nprot.2014.028

831 <https://www.nature.com/articles/nprot.2014.028#supplementary-information>, 2014.

832 Bijma, J., Hönisch, B., and Zeebe, R. E.: Impact of the ocean carbonate chemistry on living
833 foraminiferal shell weight: Comment on “Carbonate ion concentration in glacial-age deep
834 waters of the Caribbean Sea” by W. S. Broecker and E. Clark, Geochemistry, Geophysics,
835 Geosystems, 3, 1-7, 10.1029/2002GC000388, 2002.

836 Bolton, C. T., Hernandez-Sanchez, M. T., Fuertes, M.-A., Gonzalez-Lemos, S., Abrevaya, L.,
837 Mendez-Vicente, A., Flores, J.-A., Probert, I., Giosan, L., Johnson, J., and Stoll, H. M.: Decrease
838 in coccolithophore calcification and CO₂ since the middle Miocene, Nat Commun, 7,
839 10.1038/ncomms10284, 2016.

840 Böning, C. W., Dispert, A., Visbeck, M., Rintoul, S. R., and Schwarzkopf, F. U.: The response of
841 the Antarctic Circumpolar Current to recent climate change, Nature Geoscience, 1, 864,
842 10.1038/ngeo362

843 <https://www.nature.com/articles/ngeo362#supplementary-information>, 2008.

844 Bowie, A. R., Brian Griffiths, F., Dehairs, F., and Trull, T.: Oceanography of the subantarctic and
845 Polar Frontal Zones south of Australia during summer: Setting for the SAZ-Sense study, Deep
846 Sea Research Part II: Topical Studies in Oceanography, 58, 2059-2070,
847 <http://dx.doi.org/10.1016/j.dsr2.2011.05.033>, 2011.

848 Boyd, P. W.: Environmental factors controlling phytoplankton processes in the Southern
849 Ocean, Journal of Phycology, 38, 844-861, 10.1046/j.1529-8817.2002.t01-1-01203.x, 2002.

850 Boyd, P. W., and Trull, T. W.: Understanding the export of biogenic particles in oceanic waters:
851 Is there consensus?, Progress in Oceanography, 72, 276-312,
852 <http://dx.doi.org/10.1016/j.pocean.2006.10.007>, 2007.

853 Broerse, A. T. C., Ziveri, P., and Honjo, S.: Coccolithophore (–CaCO₃) flux in the Sea of Okhotsk:
854 seasonality, settling and alteration processes, Marine Micropaleontology, 39, 179-200,
855 [https://doi.org/10.1016/S0377-8398\(00\)00020-7](https://doi.org/10.1016/S0377-8398(00)00020-7), 2000a.

856 Broerse, A. T. C., Ziveri, P., van Hinte, J. E., and Honjo, S.: Coccolithophore export production,
857 species composition, and coccolith-CaCO₃ fluxes in the NE Atlantic (34°N21°W and 48°N21°W),
858 Deep Sea Research Part II: Topical Studies in Oceanography, 47, 1877-1905,
859 [https://doi.org/10.1016/S0967-0645\(00\)00010-2](https://doi.org/10.1016/S0967-0645(00)00010-2), 2000b.

860 Broerse, A. T. C., Tyrrell, T., Young, J. R., Poulton, A. J., Merico, A., Balch, W. M., and Miller, P.
861 I.: The cause of bright waters in the Bering Sea in winter, Continental Shelf Research, 23, 1579-
862 1596, <https://doi.org/10.1016/j.csr.2003.07.001>, 2003.

863 Buitenhuis, E. T., Wal, P., and Baar, H. J. W.: Blooms of *Emiliana huxleyi* are sinks of
864 atmospheric carbon dioxide: A field and mesocosm study derived simulation, Global
865 Biogeochemical Cycles, 15, 577-587, doi:10.1029/2000GB001292, 2001.

866 Buitenhuis, E. T., Pangerc, T., Franklin, D. J., Le Quéré, C., and Malin, G.: Growth rates of six
867 coccolithophorid strains as a function of temperature, 53, 1181-1185,
868 doi:10.4319/lo.2008.53.3.1181, 2008.

869 Calbet, A., Trepát, I., Almeda, R., Salá, V., Saiz, E., Movilla, J. I., Alcaraz, M., Yebra, L., and
870 Simó, R.: Impact of micro- and nanograzers on phytoplankton assessed by standard and
871 size-fractionated dilution grazing experiments, *Aquatic Microbial Ecology*, 50, 145-156, 2008.

872 Cao, L., and Caldeira, K.: Atmospheric CO₂ stabilization and ocean acidification, *Geophysical
873 Research Letters*, 35, n/a-n/a, 10.1029/2008GL035072, 2008.

874 Chang, F. H., and Gall, M.: Phytoplankton assemblages and photosynthetic pigments during
875 winter and spring in the Subtropical Convergence region near New Zealand, *New Zealand
876 Journal of Marine and Freshwater Research*, 32, 515-530, 10.1080/00288330.1998.9516840,
877 1998.

878 Chang, F. H., and Northcote, L.: Species composition of extant coccolithophores including
879 twenty six new records from the southwest Pacific near New Zealand, *Marine Biodiversity
880 Records*, 9, 75, 10.1186/s41200-016-0077-7, 2016.

881 Charalampopoulou, A., Poulton, A. J., Bakker, D. C., Lucas, M. I., Stinchcombe, M. C., and
882 Tyrrell, T. J. B.: Environmental drivers of coccolithophore abundance and calcification across
883 Drake Passage (Southern Ocean), 13, 5917-5935, 2016.

884 Chiswell, S. M., Bostock, H. C., Sutton, P. J. H., and Williams, M. J. M.: Physical oceanography of
885 the deep seas around New Zealand: a review, *New Zealand Journal of Marine and Freshwater
886 Research*, 49, 286-317, 10.1080/00288330.2014.992918, 2015.

887 Cook, S. S., Jones, R. C., Vaillancourt, R. E., and Hallegraeff, G. M.: Genetic differentiation
888 among Australian and Southern Ocean populations of the ubiquitous coccolithophore
889 *Emiliania huxleyi* (Haptophyta), *Phycologia*, 52, 368-374, 10.2216/12-111.1, 2013.

890 Cubillos, J., Wright, S., Nash, G., De Salas, M., Griffiths, B., Tilbrook, B., Poisson, A., and
891 Hallegraeff, G.: Calcification morphotypes of the coccolithophorid *Emiliania huxleyi* in the
892 Southern Ocean: changes in 2001 to 2006 compared to historical data, *Marine Ecology
893 Progress Series*, 348, 47-54, 2007.

894 D'Amario, B., Ziveri, P., Grelaud, M., and Oviedo, A.: *Emiliania huxleyi* coccolith calcite mass
895 modulation by morphological changes and ecology in the Mediterranean Sea, *PLOS ONE*, 13,
896 e0201161, 10.1371/journal.pone.0201161, 2018.

897 Daniels, C. J., Poulton, A. J., Young, J. R., Esposito, M., Humphreys, M. P., Ribas-Ribas, M.,
898 Tynan, E., and Tyrrell, T.: Species-specific calcite production reveals *Coccolithus pelagicus* as
899 the key calcifier in the Arctic Ocean, *Marine Ecology Progress Series*, 555, 29-47, 2016.

900 de Salas, M. F., Eriksen, R., Davidson, A. T., and Wright, S. W.: Protistan communities in the
901 Australian sector of the Sub-Antarctic Zone during SAZ-Sense, *Deep Sea Research Part II:
902 Topical Studies in Oceanography*, 58, 2135-2149,
903 <http://dx.doi.org/10.1016/j.dsr2.2011.05.032>, 2011.

904 Deppeler, S. L., and Davidson, A. T.: Southern Ocean Phytoplankton in a Changing Climate,
905 *Frontiers in Marine Science*, 4, 10.3389/fmars.2017.00040, 2017.

906 Diner, R. E., Benner, I., Passow, U., Komada, T., Carpenter, E. J., and Stillman, J. H. J. M. B.:
907 Negative effects of ocean acidification on calcification vary within the coccolithophore genus
908 *Calcidiscus*, 162, 1287-1305, 10.1007/s00227-015-2669-x, 2015.

909 Dugdale, R. C., Wilkerson, F. P., and Minas, H. J.: The role of a silicate pump in driving new
910 production, *Deep Sea Research Part I: Oceanographic Research Papers*, 42, 697-719,
911 [http://dx.doi.org/10.1016/0967-0637\(95\)00015-X](http://dx.doi.org/10.1016/0967-0637(95)00015-X), 1995.

912 Ebersbach, F., Trull, T. W., Davies, D. M., and Bray, S. G.: Controls on mesopelagic particle
913 fluxes in the Sub-Antarctic and Polar Frontal Zones in the Southern Ocean south of Australia in
914 summer—Perspectives from free-drifting sediment traps, *Deep Sea Research Part II: Topical
915 Studies in Oceanography*, 58, 2260-2276, <http://dx.doi.org/10.1016/j.dsr2.2011.05.025>, 2011.

916 Eriksen, R., Trull, T. W., Davies, D., Jansen, P., Davidson, A. T., Westwood, K., and van den
917 Enden, R.: Seasonal succession of phytoplankton community structure from autonomous

918 sampling at the Australian Southern Ocean Time Series (SOTS) observatory, *Marine Ecology*
919 *Progress Series*, 589, 13-31, 2018.

920 Fabry, V. J., Seibel, B. A., Feely, R. A., and Orr, J. C.: Impacts of ocean acidification on marine
921 fauna and ecosystem processes, *ICES Journal of Marine Science*, 65, 414-432,
922 10.1093/icesjms/fsn048, 2008.

923 Fabry, V. J., McClintock, J. B., Mathis, J. T., and Grebmeier, J. M.: Ocean acidification at high
924 latitudes: the bellweather, *Oceanography*, 22, 160, 2009.

925 Feng, Y., Roleda, M. Y., Armstrong, E., Boyd, P. W., and Hurd, C. L.: Environmental controls on
926 the growth, photosynthetic and calcification rates of a Southern Hemisphere strain of the
927 coccolithophore *Emiliana huxleyi*, *Limnology and Oceanography*, 62, 519-540,
928 10.1002/lno.10442, 2017.

929 Fernandez, D., Bowen, M., and Carter, L.: Intensification and variability of the confluence of
930 subtropical and subantarctic boundary currents east of New Zealand, *Journal of Geophysical*
931 *Research: Oceans*, 119, 1146-1160, 10.1002/2013jc009153, 2014.

932 Findlay, C. S., and Giraudeau, J.: Extant calcareous nannoplankton in the Australian Sector of
933 the Southern Ocean (austral summers 1994 and 1995), *Marine Micropaleontology*, 40, 417-
934 439, [http://dx.doi.org/10.1016/S0377-8398\(00\)00046-3](http://dx.doi.org/10.1016/S0377-8398(00)00046-3), 2000.

935 Fiorini, S., Middelburg, J. J., and Gattuso, J.-P.: Testing the effects of elevated pCO₂ on
936 coccolithophores (Prymnesiophyceae): comparison between haploid and diploid life stages, 47,
937 1281-1291, doi:10.1111/j.1529-8817.2011.01080.x, 2011.

938 Flores, J. A., and Sierro, F. J.: A revised technique for the calculation of calcareous nannofossil
939 accumulation rates., *Micropaleontology*, 43, 321-324, 1997.

940 Fritz, J. J., and Balch, W. M.: A light-limited continuous culture study of *Emiliana huxleyi*:
941 determination of coccolith detachment and its relevance to cell sinking, *Journal of*
942 *Experimental Marine Biology and Ecology*, 207, 127-147, [https://doi.org/10.1016/S0022-](https://doi.org/10.1016/S0022-0981(96)02633-0)
943 [0981\(96\)02633-0](https://doi.org/10.1016/S0022-0981(96)02633-0), 1996.

944 Fritz, J. J.: Carbon fixation and coccolith detachment in the coccolithophore *Emiliana huxleyi* in
945 nitrate-limited cyclostats, *Marine Biology*, 133, 509-518, 10.1007/s002270050491, 1999.

946 Fuertes, M.-Á., Flores, J.-A., and Sierro, F. J.: The use of circularly polarized light for biometry,
947 identification and estimation of mass of coccoliths, *Marine Micropaleontology*, 113, 44-55,
948 <http://dx.doi.org/10.1016/j.marmicro.2014.08.007>, 2014.

949 Gattuso, J.-P., and Hansson, L.: *Ocean acidification*, Oxford University Press, 2011.

950 Gibbs, S. J., Poulton, A. J., Bown, P. R., Daniels, C. J., Hopkins, J., Young, J. R., Jones, H. L.,
951 Thiemann, G. J., O'Dea, S. A., and Newsam, C.: Species-specific growth response of
952 coccolithophores to Palaeocene–Eocene environmental change, *Nature Geoscience*, 6, 218,
953 10.1038/ngeo1719
954 <https://www.nature.com/articles/ngeo1719#supplementary-information>, 2013.

955 Gille, S. T.: Warming of the Southern Ocean Since the 1950s, *Science*, 295, 1275-1277,
956 10.1126/science.1065863, 2002.

957 González Lemos, S., Guitián, J., Fuertes, M.-Á., Flores, J.-A., and Stoll, H. M.: An empirical
958 method for absolute calibration of coccolith thickness, *Biogeosciences*, 15, 2018.

959 Gordon, H. R., Boynton, G. C., Balch, W. M., Groom, S. B., Harbour, D. S., and Smyth, T. J.:
960 Retrieval of coccolithophore calcite concentration from SeaWiFS Imagery, *Geophysical*
961 *Research Letters*, 28, 1587-1590, 10.1029/2000gl012025, 2001.

962 Gordon, H. R., and Du, T.: Light scattering by nonspherical particles: Application to coccoliths
963 detached from *Emiliana huxleyi*, *Limnology and Oceanography*, 46, 1438-1454,
964 10.4319/lno.2001.46.6.1438, 2001.

965 Gravalosa, J. M., Flores, J.-A., Sierro, F. J., and Gersonde, R.: Sea surface distribution of
966 coccolithophores in the eastern Pacific sector of the Southern Ocean (Bellingshausen and
967 Amundsen Seas) during the late austral summer of 2001, *Marine Micropaleontology*, 69, 16-
968 25, <https://doi.org/10.1016/j.marmicro.2007.11.006>, 2008.

969 Herraiz-Borreguero, L., and Rintoul, S. R.: Regional circulation and its impact on upper ocean
970 variability south of Tasmania, *Deep Sea Research Part II: Topical Studies in Oceanography*, 58,
971 2071-2081, <http://dx.doi.org/10.1016/j.dsr2.2011.05.022>, 2011.

972 Holligan, P. M., Charalampopoulou, A., and Hutson, R.: Seasonal distributions of the
973 coccolithophore, *Emiliania huxleyi*, and of particulate inorganic carbon in surface waters of the
974 Scotia Sea, *Journal of Marine Systems*, 82, 195-205,
975 <http://dx.doi.org/10.1016/j.jmarsys.2010.05.007>, 2010.

976 Honjo, S., Manganini, S. J., Krishfield, R. A., and Francois, R.: Particulate organic carbon fluxes
977 to the ocean interior and factors controlling the biological pump: A synthesis of global
978 sediment trap programs since 1983, *Progress in Oceanography*, 76, 217-285,
979 <http://dx.doi.org/10.1016/j.pocean.2007.11.003>, 2008.

980 Hopkins, J., Henson, S. A., Painter, S. C., Tyrrell, T., and Poulton, A. J.: Phenological
981 characteristics of global coccolithophore blooms, *Global Biogeochemical Cycles*, 29, 239-253,
982 10.1002/2014GB004919, 2015.

983 King, A. L., and Howard, W. R.: Planktonic foraminiferal flux seasonality in Subantarctic
984 sediment traps: A test for paleoclimate reconstructions, *Paleoceanography*, 18, 1019,
985 10.1029/2002pa000839, 2003.

986 Kopczynska, E. E., Dehairs, F., Elskens, M., and Wright, S.: Phytoplankton and
987 microzooplankton variability between the Subtropical and Polar Fronts south of Australia:
988 Thriving under regenerative and new production in late summer, *Journal of Geophysical*
989 *Research: Oceans*, 106, 31597-31609, 10.1029/2000JC000278, 2001.

990 Krumhardt, K. M., Lovenduski, N. S., Iglesias-Rodriguez, M. D., and Kleypas, J. A.:
991 Coccolithophore growth and calcification in a changing ocean, *Progress in Oceanography*, 159,
992 276-295, <https://doi.org/10.1016/j.pocean.2017.10.007>, 2017.

993 Langdon, C., and Atkinson, M. J.: Effect of elevated pCO₂ on photosynthesis and calcification of
994 corals and interactions with seasonal change in temperature/irradiance and nutrient
995 enrichment, *Journal of Geophysical Research: Oceans*, 110, n/a-n/a, 10.1029/2004JC002576,
996 2005.

997 Langer, G., Geisen, M., Baumann, K.-H., Kläs, J., Riebesell, U., Thoms, S., and Young, J. R.:
998 Species-specific responses of calcifying algae to changing seawater carbonate chemistry,
999 *Geochemistry, Geophysics, Geosystems*, 7, n/a-n/a, 10.1029/2005GC001227, 2006.

1000 Langer, G., Nehrke, G., Probert, I., Ly, J., and Ziveri, P.: Strain-specific responses of *Emiliania*
1001 *huxleyi* to changing seawater carbonate chemistry, *Biogeosciences*, 6, 2637-2646, 2009.

1002 Langer, G., and Bode, M. J. G., *Geophysics, Geosystems: CO₂ mediation of adverse effects of*
1003 *seawater acidification in *Calcidiscus leptoporus**, 12, 2011.

1004 Lannuzel, D., Bowie, A. R., Remenyi, T., Lam, P., Townsend, A., Ibsanmi, E., Butler, E., Wagener,
1005 T., and Schoemann, V.: Distributions of dissolved and particulate iron in the sub-Antarctic and
1006 Polar Frontal Southern Ocean (Australian sector), *Deep Sea Research Part II: Topical Studies in*
1007 *Oceanography*, 58, 2094-2112, <http://dx.doi.org/10.1016/j.dsr2.2011.05.027>, 2011.

1008 Law, C. S., Schwarz, J. N., Chang, F. H., Nodder, S. D., Northcote, L. C., Safi, K. A., Marriner, A.,
1009 R.J., L., LaRoche, J., Amosa, P., van Kooten, M., Feng, Y.-Y., Rowden, A. A., and Summerfield, T.
1010 C.: Predicting changes in plankton biodiversity & productivity of the EEZ in response to climate
1011 change induced ocean acidification, Ministry for Primary Industrie, Wellington, New Zealand,
1012 200, 2014.

1013 Lawrence, C., and Menden-Deuer, S.: Drivers of protistan grazing pressure: seasonal signals of
1014 plankton community composition and environmental conditions, *Marine Ecology Progress*
1015 *Series*, 459, 39-52, 2012.

1016 Le Quéré, C., Rödenbeck, C., Buitenhuis, E. T., Conway, T. J., Langenfelds, R., Gomez, A.,
1017 Labuschagne, C., Ramonet, M., Nakazawa, T., Metzl, N., Gillett, N., and Heimann, M.:
1018 Saturation of the Southern Ocean CO₂ sink due to recent climate change, *Science*, 316, 1735-
1019 1738, 10.1126/science.1136188, 2007.

1020 Malinverno, E., Triantaphyllou, M. V., and Dimiza, M. D.: Coccolithophore assemblage
1021 distribution along a temperate to polar gradient in the West Pacific sector of the Southern
1022 Ocean (January 2005), *Micropaleontology*, 61, 489–506, 2015.

1023 Mayers, K. M. J., Poulton, A. J., Daniels, C. J., Wells, S. R., Woodward, E. M. S., Tarran, G. A.,
1024 Widdicombe, C. E., Mayor, D. J., Atkinson, A., and Giering, S. L. C.: Growth and mortality of
1025 coccolithophores during spring in a temperate Shelf Sea (Celtic Sea, April 2015), *Progress in*
1026 *Oceanography*, 177, 101928, <https://doi.org/10.1016/j.pocean.2018.02.024>, 2019.

1027 McIntyre, A., and Bé, A. W. H.: Modern coccolithophoridae of the Atlantic Ocean—I. Placoliths
1028 and cyrtoliths, *Deep Sea Research and Oceanographic Abstracts*, 14, 561-597,
1029 [https://doi.org/10.1016/0011-7471\(67\)90065-4](https://doi.org/10.1016/0011-7471(67)90065-4), 1967.

1030 McNeil, B. I., and Matear, R. J.: Southern Ocean acidification: A tipping point at 450-ppm
1031 atmospheric CO₂, *Proceedings of the National Academy of Sciences*, 105, 18860-18864, 2008.

1032 Medlin, L. K., Lange, M., and Baumann, M. E. M.: Genetic differentiation among three colony-
1033 forming species of *Phaeocystis*: further evidence for the phylogeny of the Prymnesiophyta,
1034 *Phycologia*, 33, 199-212, 10.2216/i0031-8884-33-3-199.1, 1994.

1035 Meyer, J., and Riebesell, U.: Reviews and Syntheses: Responses of coccolithophores to ocean
1036 acidification: a meta-analysis, *Biogeosciences (BG)*, 12, 1671-1682, 2015.

1037 Moy, A. D., Howard, W. R., Bray, S. G., and Trull, T. W.: Reduced calcification in modern
1038 Southern Ocean planktonic foraminifera, *Nature Geosci*, 2, 276-280,
1039 http://www.nature.com/ngeo/journal/v2/n4/supinfo/ngeo460_S1.html, 2009.

1040 Müller, M. N., Trull, T. W., and Hallegraeff, G. M.: Differing responses of three Southern Ocean
1041 *Emiliana huxleyi* ecotypes to changing seawater carbonate chemistry, *Marine Ecology*
1042 *Progress Series*, 531, 81-90, 2015.

1043 Neukermans, G., Oziel, L., and Babin, M.: Increased intrusion of warming Atlantic water leads
1044 to rapid expansion of temperate phytoplankton in the Arctic, *Global Change Biology*, 24, 2545-
1045 2553, 10.1111/gcb.14075, 2018.

1046 Nodder, S. D., Chiswell, S. M., and Northcote, L. C.: Annual cycles of deep-ocean
1047 biogeochemical export fluxes in subtropical and subantarctic waters, southwest Pacific Ocean,
1048 *Journal of Geophysical Research: Oceans*, n/a-n/a, 10.1002/2015JC011243, 2016.

1049 Northcote, L. C., and Neil, H. L.: Seasonal variations in foraminiferal flux in the Southern Ocean,
1050 Campbell Plateau, New Zealand, *Marine Micropaleontology*, 56, 122–137, 2005.

1051 O’Dea, S. A., Gibbs, S. J., Bown, P. R., Young, J. R., Poulton, A. J., Newsam, C., and Wilson, P. A.:
1052 Coccolithophore calcification response to past ocean acidification and climate change, *Nature*
1053 *Communications*, 5, 5363, 10.1038/ncomms6363

1054 <https://www.nature.com/articles/ncomms6363#supplementary-information>, 2014.

1055 Orr, J. C., Fabry, V. J., Aumont, O., Bopp, L., Doney, S. C., Feely, R. A., Gnanadesikan, A., Gruber,
1056 N., Ishida, A., and Joos, F.: Anthropogenic ocean acidification over the twenty-first century and
1057 its impact on calcifying organisms, *Nature*, 437, 681-686, 2005.

1058 Orsi, A. H., Whitworth Iii, T., and Nowlin Jr, W. D.: On the meridional extent and fronts of the
1059 Antarctic Circumpolar Current, *Deep Sea Research Part I: Oceanographic Research Papers*, 42,
1060 641-673, [http://dx.doi.org/10.1016/0967-0637\(95\)00021-W](http://dx.doi.org/10.1016/0967-0637(95)00021-W), 1995.

1061 Paasche, E.: Coccolith Formation, *Nature*, 193, 1094-1095, 10.1038/1931094b0, 1962.

1062 Paasche, E.: A review of the coccolithophorid *Emiliana huxleyi* (Prymnesiophyceae), with
1063 particular reference to growth, coccolith formation, and calcification-photosynthesis
1064 interactions, *Phycologia*, 40, 503-529, 10.2216/i0031-8884-40-6-503.1, 2002.

1065 Pachauri, R. K., Allen, M. R., Barros, V. R., Broome, J., Cramer, W., Christ, R., Church, J. A.,
1066 Clarke, L., Dahe, Q., and Dasgupta, P.: Climate change 2014: synthesis report. Contribution of
1067 Working Groups I, II and III to the fifth assessment report of the Intergovernmental Panel on
1068 Climate Change, *Ipcc*, 2014.

1069 Passow, U., and De La Rocha, C. L.: Accumulation of mineral ballast on organic aggregates,
1070 *Global Biogeochemical Cycles*, 20, GB1013, 10.1029/2005GB002579, 2006.

1071 Patarnello, T., Bargelloni, L., Varotto, V., and Battaglia, B.: Krill evolution and the Antarctic
1072 ocean currents: evidence of vicariant speciation as inferred by molecular data, *Marine Biology*,
1073 126, 603-608, 10.1007/bf00351327, 1996.

1074 Patil, S. M., Mohan, R., Shetye, S. S., Gazi, S., Baumann, K.-H., and Jafar, S.: Biogeographic
1075 distribution of extant Coccolithophores in the Indian sector of the Southern Ocean, *Marine*
1076 *Micropaleontology*, 137, 16-30, <https://doi.org/10.1016/j.marmicro.2017.08.002>, 2017.

1077 Poulton, A. J., Charalampopoulou, A., Young, J. R., Tarran, G. A., Lucas, M. I., and Quartly, G.
1078 D.: Coccolithophore dynamics in non-bloom conditions during late summer in the central
1079 Iceland Basin (July-August 2007), *Limnology and Oceanography*, 55, 1601-1613,
1080 10.4319/lo.2010.55.4.1601, 2010.

1081 Poulton, A. J., Young, J. R., Bates, N. R., and Balch, W. M.: Biometry of detached *Emiliania*
1082 *huxleyi* coccoliths along the Patagonian Shelf, *Marine Ecology Progress Series*, 443, 1-17, 2011.

1083 Poulton, A. J., Painter, S. C., Young, J. R., Bates, N. R., Bowler, B., Drapeau, D., Lyczskowski, E.,
1084 and Balch, W. M.: The 2008 *Emiliania huxleyi* bloom along the Patagonian Shelf: Ecology,
1085 biogeochemistry, and cellular calcification, *Global Biogeochemical Cycles*, 27, 1023-1033,
1086 10.1002/2013gb004641, 2013.

1087 Probert, I., and Houdan, A.: The laboratory culture of coccolithophores, in: *Coccolithophores*,
1088 Springer, 217-249, 2004.

1089 Quéguiner, B.: Iron fertilization and the structure of planktonic communities in high nutrient
1090 regions of the Southern Ocean, *Deep Sea Research Part II: Topical Studies in Oceanography*,
1091 90, 43-54, <http://dx.doi.org/10.1016/j.dsr2.2012.07.024>, 2013.

1092 Quéré, C. L., Harrison, S. P., Colin Prentice, I., Buitenhuis, E. T., Aumont, O., Bopp, L., Claustre,
1093 H., Cotrim Da Cunha, L., Geider, R., Giraud, X., Klaas, C., Kohfeld, K. E., Legendre, L., Manizza,
1094 M., Platt, T., Rivkin, R. B., Sathyendranath, S., Uitz, J., Watson, A. J., and Wolf-Gladrow, D.:
1095 Ecosystem dynamics based on plankton functional types for global ocean biogeochemistry
1096 models, *Global Change Biology*, 11, 2016-2040, 10.1111/j.1365-2486.2005.1004.x, 2005.

1097 Rigual-Hernández, A. S., Trull, T. W., Bray, S. G., Closset, I., and Armand, L. K.: Seasonal
1098 dynamics in diatom and particulate export fluxes to the deep sea in the Australian sector of
1099 the southern Antarctic Zone, *Journal of Marine Systems*, 142, 62-74,
1100 <http://dx.doi.org/10.1016/j.jmarsys.2014.10.002>, 2015a.

1101 Rigual-Hernández, A. S., Trull, T. W., Bray, S. G., Cortina, A., and Armand, L. K.: Latitudinal and
1102 temporal distributions of diatom populations in the pelagic waters of the Subantarctic and
1103 Polar Frontal Zones of the Southern Ocean and their role in the biological pump,
1104 *Biogeosciences* 12, 8615-8690, 10.5194/bg-12-8615-2015, 2015b.

1105 Rigual Hernández, A. S., Flores, J. A., Sierro, F. J., Fuertes, M. A., Cros, L., and Trull, T. W.:
1106 Coccolithophore populations and their contribution to carbonate export during an annual cycle
1107 in the Australian sector of the Antarctic zone, *Biogeosciences*, 15, 1843-1862, 10.5194/bg-15-
1108 1843-2018, 2018.

1109 Rintoul, S. R., and Trull, T. W.: Seasonal evolution of the mixed layer in the Subantarctic zone
1110 south of Australia, *Journal of Geophysical Research: Oceans*, 106, 31447-31462,
1111 10.1029/2000JC000329, 2001.

1112 Rintoul, S. R., Sparrow, M., Meredith, M. P., Wadley, V., Speer, K., Hofmann, E., Summerhayes,
1113 C., Urban, E., Bellerby, R., and Ackley, S.: The Southern Ocean observing system: initial science
1114 and implementation strategy, *Scientific Committee on Antarctic Research*, 2012.

1115 Rivero-Calle, S., Gnanadesikan, A., Del Castillo, C. E., Balch, W. M., and Guikema, S. D.:
1116 Multidecadal increase in North Atlantic coccolithophores and the potential role of rising CO₂,
1117 *Science*, 350, 1533-1537, 10.1126/science.aaa8026, 2015.

1118 Rost, B., and Riebesell, U.: Coccolithophores and the biological pump: responses to
1119 environmental changes, in: *Coccolithophores: From Molecular Processes to Global Impact*,
1120 edited by: Thierstein, H. R., and Young, J. R., Springer Berlin Heidelberg, Berlin, Heidelberg, 99-
1121 125, 2004.

1122 Rousseaux, C. S., and Gregg, W. W.: Recent decadal trends in global phytoplankton
1123 composition, *Global Biogeochemical Cycles*, 29, 1674-1688, 2015.

1124 Saavedra-Pellitero, M., Baumann, K.-H., Flores, J.-A., and Gersonde, R.: Biogeographic
1125 distribution of living coccolithophores in the Pacific sector of the Southern Ocean, *Marine*
1126 *Micropaleontology*, 109, 1-20, 2014.

1127 Saavedra-Pellitero, M., and Baumann, K.-H.: Comparison of living and surface sediment
1128 coccolithophore assemblages in the Pacific sector of the Southern Ocean, *Micropaleontology*,
1129 61, 507-520, 2015.

1130 Sabine, C. L., Feely, R. A., Gruber, N., Key, R. M., Lee, K., Bullister, J. L., Wanninkhof, R., Wong,
1131 C. S., Wallace, D. W. R., Tilbrook, B., Millero, F. J., Peng, T.-H., Kozyr, A., Ono, T., and Rios, A. F.:
1132 The Oceanic Sink for Anthropogenic CO₂, *Science*, 305, 367-371, 10.1126/science.1097403,
1133 2004.

1134 Salter, I., Schiebel, R., Ziveri, P., Movellan, A., Lampitt, R., and Wolff, G. A.: Carbonate counter
1135 pump stimulated by natural iron fertilization in the Polar Frontal Zone, *Nature Geosci*, 7, 885-
1136 889, 10.1038/ngeo2285

1137 [http://www.nature.com/ngeo/journal/v7/n12/abs/ngeo2285.html#supplementary-](http://www.nature.com/ngeo/journal/v7/n12/abs/ngeo2285.html#supplementary-information)
1138 [information](http://www.nature.com/ngeo/journal/v7/n12/abs/ngeo2285.html#supplementary-information), 2014.

1139 Samtleben, C., and Bickert, T.: Coccoliths in sediment traps from the Norwegian Sea, *Marine*
1140 *Micropaleontology*, 16, 39-64, [https://doi.org/10.1016/0377-8398\(90\)90028-K](https://doi.org/10.1016/0377-8398(90)90028-K), 1990.

1141 Schiebel, R., and Hemleben, C.: *Planktic foraminifers in the modern ocean*, Springer, 2017.

1142 Schiebel, R., Spielhagen, R. F., Garnier, J., Hagemann, J., Howa, H., Jentzen, A., Martínez-García,
1143 A., Meilland, J., Michel, E., Repschläger, J., Salter, I., Yamasaki, M., and Haug, G.: Modern
1144 planktic foraminifers in the high-latitude ocean, *Marine Micropaleontology*, 136, 1-13,
1145 <https://doi.org/10.1016/j.marmicro.2017.08.004>, 2017.

1146 Schlitzer, R.: *Ocean Data View*, 2018.

1147 Shadwick, E. H., Trull, T. W., Thomas, H., and Gibson, J. A. E.: Vulnerability of Polar Oceans to
1148 Anthropogenic Acidification: Comparison of Arctic and Antarctic Seasonal Cycles, *Scientific*
1149 *Reports*, 3, 2339, 10.1038/srep02339, 2013.

1150 Sinha, B., Buitenhuis, E. T., Quéré, C. L., and Anderson, T. R.: Comparison of the emergent
1151 behavior of a complex ecosystem model in two ocean general circulation models, *Progress in*
1152 *Oceanography*, 84, 204-224, <https://doi.org/10.1016/j.pocean.2009.10.003>, 2010.

1153 Sloyan, B. M., and Rintoul, S. R.: Circulation, Renewal, and Modification of Antarctic Mode and
1154 Intermediate Water, *Journal of Physical Oceanography*, 31, 1005-1030, 10.1175/1520-
1155 0485(2001)031<1005:cramoa>2.0.co;2, 2001a.

1156 Sloyan, B. M., and Rintoul, S. R.: The Southern Ocean Limb of the Global Deep Overturning
1157 Circulation, *Journal of Physical Oceanography*, 31, 143-173, 10.1175/1520-
1158 0485(2001)031<0143:TSOLOT>2.0.CO;2, 2001b.

1159 Sokolov, S., and Rintoul, S. R.: Circumpolar structure and distribution of the Antarctic
1160 Circumpolar Current fronts: 2. Variability and relationship to sea surface height, *Journal of*
1161 *Geophysical Research: Oceans*, 114, C11019, 10.1029/2008JC005248, 2009.

1162 Thornhill, D. J., Mahon, A. R., Norenburg, J. L., and Halanych, K. M.: Open-ocean barriers to
1163 dispersal: a test case with the Antarctic Polar Front and the ribbon worm *Parborlasia*
1164 *corrugatus* (Nemertea: Lineidae), *Molecular Ecology*, 17, 5104-5117, 10.1111/j.1365-
1165 294X.2008.03970.x, 2008.

1166 Trull, T. W., Bray, S. G., Manganini, S. J., Honjo, S., and François, R.: Moored sediment trap
1167 measurements of carbon export in the Subantarctic and Polar Frontal zones of the Southern
1168 Ocean, south of Australia, *Journal of Geophysical Research: Oceans*, 106, 31489-31509,
1169 10.1029/2000JC000308, 2001.

1170 Trull, T. W., Schulz, E., Bray, S. G., Pender, L., McLaughlan, D., Tilbrook, B., Rosenberg, M., and
1171 Lynch, T.: The Australian Integrated Marine Observing System Southern Ocean Time Series
1172 facility, *OCEANS 2010 IEEE - Sydney*, 2010, 1-7,

1173 Trull, T. W., Passmore, A., Davies, D. M., Smit, T., Berry, K., and Tilbrook, B.: The distribution of
1174 pelagic biogenic carbonates in the Southern Ocean south of Australia: a baseline for ocean
1175 acidification impact assessment, *Biogeosciences*, in press, 2018.

1176 Tyrrell, T., and Merico, A.: *Emiliana huxleyi*: bloom observations and the conditions that
1177 induce them, in: *Coccolithophores*, Springer, 75-97, 2004.

1178 Volk, T., and Hoffert, M. I.: Ocean Carbon Pumps: Analysis of Relative Strengths and
1179 Efficiencies in Ocean-Driven Atmospheric CO₂ Changes, in: *The Carbon Cycle and Atmospheric*
1180 *CO₂: Natural Variations Archean to Present*, 99-110, 1985.

1181 Winter, A., Henderiks, J., Beaufort, L., Rickaby, R. E., and Brown, C. W.: Poleward expansion of
1182 the coccolithophore *Emiliana huxleyi*, *Journal of Plankton Research*, 36, 316-325, 2014.

1183 Young, J., Geisen, M., Cross, L., Kleijne, A., Sprengel, C., Probert, I., and Østergaard, J.: A guide
1184 to extant coccolithophore taxonomy, *Journal of Nanoplankton Research Special Issue 1*,
1185 International Nannoplankton Association, 2003.

1186 Young, J. R.: The description and analysis of coccolith structure, *Nannoplankton Research*.
1187 Hamrsmid B, Young JR (eds) ZPZ, Knihovnichá, 35-71, 1992.

1188 Young, J. R., Davis, S. A., Bown, P. R., and Mann, S.: Coccolith Ultrastructure and
1189 Biomineralisation, *Journal of Structural Biology*, 126, 195-215,
1190 <https://doi.org/10.1006/jsbi.1999.4132>, 1999.

1191 Young, J. R., and Ziveri, P.: Calculation of coccolith volume and its use in calibration of carbonate
1192 flux estimates, *Deep Sea Research Part II: Topical Studies in Oceanography*, 47, 1679-1700,
1193 [http://dx.doi.org/10.1016/S0967-0645\(00\)00003-5](http://dx.doi.org/10.1016/S0967-0645(00)00003-5), 2000.

1194 Nannotax3 website: <http://www.mikrotax.org/Nannotax3> access: July 2019, 2019.

1195 Zhang, X., Lewis, M., Lee, M., Johnson, B., and Korotaev, G.: The volume scattering function of
1196 natural bubble populations, *Limnology and Oceanography*, 47, 1273-1282, 2002.

1197 Ziveri, P., Broerse, A. T. C., van Hinte, J. E., Westbroek, P., and Honjo, S.: The fate of coccoliths
1198 at 48°N 21°W, Northeastern Atlantic, *Deep Sea Research Part II: Topical Studies in*
1199 *Oceanography*, 47, 1853-1875, [http://dx.doi.org/10.1016/S0967-0645\(00\)00009-6](http://dx.doi.org/10.1016/S0967-0645(00)00009-6), 2000.

1200 Ziveri, P., de Bernardi, B., Baumann, K.-H., Stoll, H. M., and Mortyn, P. G.: Sinking of coccolith
1201 carbonate and potential contribution to organic carbon ballasting in the deep ocean, *Deep Sea*
1202 *Research Part II: Topical Studies in Oceanography*, 54, 659-675,
1203 <http://dx.doi.org/10.1016/j.dsr2.2007.01.006>, 2007.

1204